

Shor–Laflamme distributions of graph states and noise robustness of entanglement

Daniel Miller^{1,2,3,4,*} , Daniel Loss² , Ivano Tavernelli³ ,
Hermann Kampermann⁴ , Dagmar Bruß⁴
and Nikolai Wyderka⁴ 

¹ Freie Universität Berlin, Dahlem Center for Complex Quantum Systems, 14195 Berlin, Germany

² Department of Physics, Universität Basel, Klingelbergstrasse 82, CH-4056 Basel, Switzerland

³ IBM Quantum, IBM Research Europe—Zurich, Säumerstrasse 4, CH-8803 Rüschlikon, Switzerland

⁴ Heinrich-Heine-Universität Düsseldorf, Institut für Theoretische Physik III, Universitätsstraße 1, DE-40225 Düsseldorf, Germany

E-mail: d.miller@fu-berlin.de

Received 12 January 2023; revised 13 June 2023

Accepted for publication 19 July 2023

Published 31 July 2023



CrossMark

Abstract

The Shor–Laflamme distribution (SLD) of a quantum state is a collection of local unitary invariants that quantify k -body correlations. We show that the SLD of graph states can be derived by solving a graph-theoretical problem. In this way, the mean and variance of the SLD are obtained as simple functions of efficiently computable graph properties. Furthermore, this formulation enables us to derive closed expressions of SLDs for some graph state families. For cluster states, we observe that the SLD is very similar to a binomial distribution, and we argue that this property is typical for graph states in general. Finally, we derive an SLD-based entanglement criterion from the purity criterion and apply it to derive meaningful noise thresholds for entanglement. Our new entanglement criterion is easy to use and also applies to the case of higher-dimensional qudits. In the bigger picture, our results foster the understanding both of quantum error-correcting codes, where a closely related notion of SLDs

* Author to whom any correspondence should be addressed.



Original Content from this work may be used under the terms of the [Creative Commons Attribution 4.0 licence](https://creativecommons.org/licenses/by/4.0/). Any further distribution of this work must maintain attribution to the author(s) and the title of the work, journal citation and DOI.

plays an important role, and of the geometry of quantum states, where SLDs are known as sector length distributions.

Keywords: Shor–Laflamme distributions, sector length distributions, graph states, stabilizer formalism, quantum entanglement, noisy entangled states, quantum error correction

(Some figures may appear in colour only in the online journal)

Contents

1. Introduction	2
1.1. Relevance of our developments	3
1.2. Setting the stage	4
1.3. Outline of our paper	4
2. Graph-theoretical formulation for SLDs	4
2.1. General insights	6
2.2. Formulae for mean and variance of normalized SLDs	7
2.3. Analytical SLDs of various families of graph states	9
3. Numerical investigation of SLDs of graph states	11
3.1. SLDs of cluster states	12
3.2. SLDs of random graph states	13
4. Generalization to higher-dimensional qudits	15
4.1. Known results about SLDs of qudit states	16
4.2. A novel entanglement criterion for multi-qudit states based on SLDs	17
5. SLDs of noisy states	18
5.1. The impact of noise on qudit SLDs	18
5.2. Lower bounds on entanglement noise thresholds	19
6. Conclusion and outlook	21
Data availability statement	21
Acknowledgments	21
Appendix A. Solution of the graph-theoretical problem for the Pusteblume graph	22
Appendix B. Solution of the graph-theoretical problem for the cycle graph	23
Appendix C. Lower bounds on entanglement noise thresholds of graph states	27
C.1. Robustness of entanglement in qubit graph states against local white noise	27
C.2. Robustness of entanglement in qudit graph states against local white noise	28
Appendix D. SLDs of W states as an example of the non-stabilizer case	29
Appendix E. Expected SLD for random graph states	31
Appendix F. Graph-theoretical treatment of SLDs of qudit graph states	32
Appendix G. Proof of theorem 4	34
References	36

1. Introduction

In the quest toward fault-tolerant quantum computation, *quantum error-correcting codes* (QECCs) are taking the main stage. A thorough understanding of QECCs is central to the eventual success of realizing error-corrected quantum computers. In a landmark paper of 1997,

Peter Shor and Raymond Laflamme pointed out that certain numerical invariants are particularly useful to characterize a QECC [1]. Their idea is most easily explained for the special case of a stabilizer QECC [2], which is defined via a stabilizer subgroup \mathcal{S} of the n -qubit Pauli group $\mathcal{P}^n = \{i^q X^{\mathbf{r}} Z^{\mathbf{s}} \mid q \in \mathbb{Z}/4\mathbb{Z}, \mathbf{r}, \mathbf{s} \in \mathbb{F}_2^n\}$, where $\mathbb{F}_2 = \{0, 1\}$ is the binary field and a Pauli operator $X^{\mathbf{r}} Z^{\mathbf{s}}$ is defined via its action $X^{\mathbf{r}} Z^{\mathbf{s}} |\mathbf{b}\rangle = (-1)^{\mathbf{b} \cdot \mathbf{s}} |\mathbf{b} + \mathbf{r}\rangle$ on computational basis states $|\mathbf{b}\rangle \in (\mathbb{C}^2)^{\otimes n}$. For a stabilizer group \mathcal{S} , Shor and Laflamme define for each $k \in \{0, \dots, n\}$ the integers

$$A_k(\mathcal{S}) = |\{S \in \mathcal{S} \mid \text{wt}(S) = k\}| \tag{1}$$

$$\text{and } B_k(\mathcal{S}) = |\{P \in \mathcal{N}(\mathcal{S})/\sim \mid \text{wt}(P) = k\}|, \tag{2}$$

where $\mathcal{N}(\mathcal{S}) = \{P \in \mathcal{P}^n \mid \forall S \in \mathcal{S} : PSP^\dagger \in \mathcal{S}\}$ is the normalizer of \mathcal{S} in the Pauli group, and $\mathcal{N}(\mathcal{S})/\sim$ is the normalizer modulo global phases. In other words, $A_k(\mathcal{S})$ counts Pauli operators $X^{\mathbf{r}} Z^{\mathbf{s}}$ acting as the logical identity on the QECC for which the Pauli weight $\text{wt}(X^{\mathbf{r}} Z^{\mathbf{s}}) = |\{i \in \{1, \dots, n\} \mid r_i = 1 \vee s_i = 1\}|$ is equal to k . Similarly, $B_k(\mathcal{S})$ counts weight- k Pauli operators that act as any logical operations on the QECC. In particular, we have $A_k(\mathcal{S}) \leq B_k(\mathcal{S})$ for all k ; the smallest integer d with $A_d(\mathcal{S}) < B_d(\mathcal{S})$ is the distance of the QECC, i.e. the smallest weight of a Pauli operator that maps some codeword of the QECC onto a different one. While the distance d is one of the most important characteristics of a QECC, it is in general notoriously difficult to compute. To tackle this problem, the quantities defined in equations (1) and (2) provide a powerful handle: first note that $d = \min\{k \geq 1 \mid A_k(\mathcal{S}) < B_k(\mathcal{S})\}$ can be reconstructed if A_k and B_k are known for all k . Strikingly, it is sufficient to know the A_k 's because, surprisingly, they uniquely determine the B_k 's through a quantum version of the MacWilliams identity [1]. This reduces the problem of computing the distance of a stabilizer QECC to counting its weight- k stabilizers, which is still challenging but at least it breaks down the problem.

1.1. Relevance of our developments

In this paper, we develop a formal approach (theorem 1) for counting weight- k stabilizers in the special case of stabilizer states [2]. On the one hand, our work should be understood as a first step toward tackling the challenge of computing the distance of stabilizer QECCs via the quantum MacWilliams identity. On the other hand, computing $A_k(\mathcal{S})$ for a stabilizer state $|\psi\rangle$ is interesting in its own right. For example, it is well known that $A_1 = A_2 = \dots = A_m = 0$ is equivalent to $|\psi\rangle$ being an m -uniform state, i.e. all m -body marginals of $|\psi\rangle$ being maximally mixed [3, 4]. This already shows that the Shor–Laflamme distribution (SLD) of a quantum state contains information about its entanglement.

As a second important contribution, we apply the purity criterion [5] to derive a new entanglement criterion (theorem 4). The new criterion is very general as it also applies to higher-dimensional qudits and non-stabilizer states. Furthermore, it allows the derivation of lower bounds on the entanglement noise threshold (corollary 5) of quantum states for which we only need to know the SLD. Importantly, all of this also works for the physically relevant case of local white noise, a noise channel with many cross terms that render many other entanglement criteria inapplicable.

Among other applications, to showcase the effectiveness of our approach, we derive the SLD of cycle graph states. This enables us to improve the best previously-known lower bound on the entanglement noise threshold of cycle graph states.

1.2. Setting the stage

Before we begin the presentation of our theory in section 2, let us briefly review a generalization of the definition in equation (1). For a general n -qubit state with density matrix ρ and every $k \in \{0, \dots, n\}$, let

$$A_k[\rho] = \sum_{\substack{\mathbf{r}, \mathbf{s} \in \mathbb{F}_2^n \\ \text{swt}(\mathbf{r}, \mathbf{s})=k}} |\text{Tr}[\rho X^{\mathbf{r}} Z^{\mathbf{s}}]|^2, \tag{3}$$

where $\text{swt}(\mathbf{r}, \mathbf{s}) = \text{wt}(X^{\mathbf{r}} Z^{\mathbf{s}})$ is the *symplectic weight* of $(\mathbf{r}, \mathbf{s}) \in \mathbb{F}_2^n \oplus \mathbb{F}_2^n$. To honor the seminal work [1] in which equation (3) was first defined, we will call

$$\mathbf{A}[\rho] = (A_0[\rho], \dots, A_n[\rho]) \in \mathbb{R}^{n+1} \tag{4}$$

the SLD of the state ρ . Note that $\mathbf{A}[\rho]$ is sometimes referred to as *sector length (SL) distribution* in the literature [1, 6–12] which conveniently has the same acronym. Because of $\text{Tr}[\rho^2] = \sum_{k=0}^n A_k[\rho]/2^n$, the *normalized SLD* $\mathbf{a} = \mathbf{A}/2^n$ is a probability distribution, provided ρ is a pure state.

To develop the theory of SLDs of stabilizer states, we can restrict ourselves to the case of *graph states* [13, 14]

$$|\Gamma\rangle = \frac{1}{\sqrt{2^n}} \sum_{\mathbf{r}=(r_1, \dots, r_n) \in \mathbb{F}_2^n} (-1)^{\sum_{i=1}^n \sum_{j=i+1}^n r_i \gamma_{i,j} r_j} |\mathbf{r}\rangle, \tag{5}$$

which are defined via the *adjacency matrix* $\Gamma = (\gamma_{i,j})_{1 \leq i, j \leq n} \in \mathbb{F}_2^{n \times n}$ of a graph. If Γ' is a different graph (we do not distinguish between a graph and its adjacency matrix) that arises from Γ via local complementation [15], the states $|\Gamma\rangle$ and $|\Gamma'\rangle$ are local-unitary (LU) equivalent [13]. Since equation (3) is invariant under LU transformations [1], the SLDs of $|\Gamma\rangle$ and $|\Gamma'\rangle$ coincide. It is well known that every stabilizer state is LU-equivalent to some graph state [16]. For this reason, most of our results about SLDs of graph states will be directly applicable to general stabilizer states.

1.3. Outline of our paper





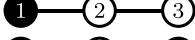



This paper is organized as follows. We begin in section 2 by formulating and investigating a graph-theoretical color assignment problem, which the SLD of the corresponding graph state solves. In section 3, we numerically examine SLDs of cluster states and random graph states. In section 4, we generalize some of our findings to SLDs of graph states for higher-dimensional qudits, and we present a simplified version of the purity criterion that can be tested already on the level of SLDs. Afterward, in section 5, we derive formulas for how SLDs change under the influence of global or local depolarizing noise, and we investigate implications for noise thresholds of entanglement. Finally, in section 6, we summarize the central results of this work and provide a short outlook about related research avenues.

2. Graph-theoretical formulation for SLDs

Every n -qubit graph state $|\Gamma\rangle$, as defined in equation (5), is a stabilizer state whose stabilizer group $\mathcal{S} = \langle S_1, \dots, S_n \rangle$ is generated by operators of the form [13, 14]

$$S_i = X^{(i)} \prod_{j=1}^n (Z^{(j)})^{\gamma_{i,j}}. \tag{6}$$

Table 1. Correspondence between black-white color assignments, binary vectors $\mathbf{r} \in \mathbb{F}_2^n$, and stabilizer operators (up to sign) $X^{\mathbf{r}}Z^{\Gamma\mathbf{r}}$ for the path-graph P_n with $n = 3$ vertices. White and black vertices correspond to zeros and ones in \mathbf{r} , respectively. Thus, every black vertex is associated with an X -operator on the corresponding qubit. Likewise, a Z -operator is induced on each neighbor of a black vertex. Since a vertex can have multiple black neighbors, the induced Z -operators may cancel, e.g. $\mathbf{r} = (1, 0, 1)$. The weight $\text{swt}(\mathbf{r}, \mathbf{s})$ of a Pauli operator $\pm X^{\mathbf{r}}Z^{\mathbf{s}}$ counts the number of non-identity tensor factors. The only possibility for $\mathbb{1}$ to occur as a tensor factor of an operator $X^{\mathbf{r}}Z^{\Gamma\mathbf{r}}$ is if the corresponding vertex is white (no X) and has an even number of black neighbors (no Z). The SLD $(A_0, A_1, A_2, A_3) = (1, 0, 3, 4)$ coincides with the Pauli-weight distribution of the operators in the stabilizer group of $|P_3\rangle$.

Color assignment	$\mathbf{r} = (r_1, r_2, r_3)$	$X^{\mathbf{r}}Z^{\Gamma\mathbf{r}}$	$\text{swt}(\mathbf{r}, \Gamma\mathbf{r})$
	(0, 0, 0)	$\mathbb{1} \otimes \mathbb{1} \otimes \mathbb{1}$	0
	(0, 0, 1)	$\mathbb{1} \otimes Z \otimes X$	2
	(0, 1, 0)	$Z \otimes X \otimes Z$	3
	(0, 1, 1)	$Z \otimes XZ \otimes XZ$	3
	(1, 0, 0)	$X \otimes Z \otimes \mathbb{1}$	2
	(1, 0, 1)	$X \otimes \mathbb{1} \otimes X$	2
	(1, 1, 0)	$XZ \otimes XZ \otimes Z$	3
	(1, 1, 1)	$XZ \otimes X \otimes XZ$	3

Therefore, every operator in \mathcal{S} can be written as

$$\prod_{i=1}^n S_i^{r_i} = \sigma_{\Gamma}(\mathbf{r}) X^{\mathbf{r}} Z^{\Gamma\mathbf{r}} \tag{7}$$

for some bit string $\mathbf{r} = (r_1, \dots, r_n) \in \mathbb{F}_2^n$. Note that the prefactor $\sigma_{\Gamma}(\mathbf{r}) = \prod_{i < j} (-1)^{r_i r_j \gamma_{ij}}$ in equation (7), which arises from the anti-commutativity relation of X and Z , is irrelevant for our purposes as we are only interested in the Pauli weight of $X^{\mathbf{r}}Z^{\Gamma\mathbf{r}}$, which is equal to the symplectic weight of $(\mathbf{r}, \Gamma\mathbf{r}) \in \mathbb{F}_2^n \oplus \mathbb{F}_2^n$. By counting all weight- k Pauli operators in \mathcal{S} , we obtain the k -body SL,

$$A_k = |\{\mathbf{r} \in \mathbb{F}_2^n \mid \text{swt}(\mathbf{r}, \Gamma\mathbf{r}) = k\}|, \tag{8}$$

of the graph state $|\Gamma\rangle$. We can interpret a given bit string $\mathbf{r} \in \mathbb{F}_2^n$ as a color assignment of the graph Γ by declaring vertex i to be white if $r_i = 0$, and black if $r_i = 1$. The symplectic weight of $(\mathbf{r}, \Gamma\mathbf{r})$ is then given by the sum of the number of black vertices ($r_i = 1$) and the number of white vertices having an odd number of black neighbors ($r_i = 0$ but the i th entry of $\Gamma\mathbf{r}$ is equal to 1). In other words, we have $\text{swt}(\mathbf{r}, \Gamma\mathbf{r}) = k$ if and only if (iff) there are exactly $n - k$ white vertices with an even number of black neighbors, see table 1 for an illustrative example. This shows:

Theorem 1 (graph-theoretical formulation of SLDs). *Let $|\Gamma\rangle$ be an n -qubit graph state and $\mathbf{A} = (A_0, \dots, A_n)$ its SLD. For each $k \in \{0, \dots, n\}$, A_k is equal to the number of black-white color assignments of Γ for which exactly $n - k$ white vertices have an even number of black neighbors.*

2.1. General insights

While theorem 1 does not alleviate the exponential complexity of computing the entire SLD of an arbitrary graph state $|\Gamma\rangle$, we can exploit it to express A_k for small values of k in purely graph-theoretical terms:

In the trivial case, $k = 0$, the theorem only addresses the color assignment for which all n vertices are white; we obtain the well-known normalization condition $A_0 = 1$.

For $k = 1$, the situation is more interesting: in order for a color assignment to contribute to A_1 , there have to be $n - 1$ white vertices that are disconnected from the black vertex. Thus, every color assignment with a single black, isolated vertex contributes; other color assignments do not contribute. Therefore, we find

$$A_1 = I, \tag{9}$$

where I is the number of *isolated vertices* of the graph. This number is efficiently computed as the number of rows of the adjacency matrix Γ in which all entries are equal to zero. After potentially reordering the qubits, we can write $|\Gamma\rangle = |+\rangle^{\otimes A_1} \otimes |\tilde{\Gamma}\rangle$ where $\tilde{\Gamma}$ is a graph without any isolated vertices.

To express the 2-body SL in graph-theoretical terms, we note that only color assignments with one or two black vertices can contribute to A_2 . If there is only one black vertex, it has to be connected to exactly one other (automatically white) vertex to ensure that there are exactly $n - 2$ white vertices with an even number (automatically zero) of black neighbors; thus, the black vertex has to be a *leaf*. For the color assignments with exactly two black vertices, however, all other vertices have to be connected to either both or none of the black ones. Otherwise, one of the white vertices would have an odd number of black neighbors; thus, the two black vertices must form a *twin pair*, i.e. have the same neighborhood. Therefore,

$$A_2 = L + T \tag{10}$$

is the sum of the number of leaves $L = |\{i \in \{1, \dots, n\} \mid \exists! j \in \{1, \dots, n\} : \gamma_{i,j} = 1\}|$ and the number of twin pairs $T = |\{\{i, j\} \subset \{1, \dots, n\} \mid i \neq j, \forall k \in \{1, \dots, n\} \setminus \{i, j\} : \gamma_{i,k} = \gamma_{j,k}\}|$, where ‘ $\exists!$ ’ denotes the unique existential quantification. It has been pointed out before that $L + T$ is invariant under local complementation [15]. Our interpretation of this number as the 2-body SL establishes the stronger [17, 18] fact that $L + T$ is an LU invariant of graph states.

In principle, one could continue in a similar manner and also express A_k for $k \geq 3$ in graph-theoretical terms. By counting all color assignments contributing to A_k which have exactly $b \in \{0, \dots, k\}$ black vertices, we obtain the formal expression

$$A_k = \sum_{b=0}^k \sum_{\mathbf{r} \in \mathcal{B}_b} \delta_{\text{swt}(\mathbf{r}, \Gamma \mathbf{r}), k}, \tag{11}$$

where $\mathcal{B}_b \subset \mathbb{F}_2^n$ is the subset of bit strings having a Hamming weight of b . For $k \geq 3$, however, the graph-theoretical interpretation of equation (11) becomes increasingly complicated. Nevertheless, it immediately yields that the cumulative binomial distribution is an upper bound for the k -body SL, i.e.

$$A_k[\rho] \leq \sum_{b=0}^k |\mathcal{B}_b| = \sum_{b=0}^k \binom{n}{b} \tag{12}$$

for every graph state $\rho = |\Gamma\rangle\langle\Gamma|$. Since every stabilizer state is LU-equivalent to a graph state and $A_k[\cdot]$ is convex and LU-invariant, the bound in equation (12) is also fulfilled for mixtures $\rho = \sum_i p_i |\psi_i\rangle\langle\psi_i|$ of stabilizer states $|\psi_i\rangle$. For $k \geq 1$, we can drop the term with $b = 0$ in

equation (12) because \mathcal{B}_0 only contains the trivial color assignment that contributes to A_0 but not to A_k for $k > 0$.

By equation (11), A_k can be computed with runtime $\mathcal{O}(n^k)$, which is efficient for small values of k . In the opposite case, where $k = n$, theorem 1 simplifies to the following problem: ‘ A_n is equal to the number of color assignments of Γ for which every white vertex has an odd number of black neighbors’. Hence, a color assignment $\mathbf{r} \in \mathbb{F}_2^n$ contributes to A_n iff every vertex $i \in \{1, \dots, n\}$ is either black ($r_i = 1$) or has an odd number of black neighbors ($\sum_{j=1}^n \gamma_{i,j} r_j = 1$), or both. In other words, \mathbf{r} contributes to $A_n = |\mathcal{V}|$ iff it lies in the intersection, $\mathcal{V} = \bigcap_{i=1}^n \mathcal{V}_i$, of the n quadric hypersurfaces \mathcal{V}_i that are defined as

$$\mathcal{V}_i = \left\{ \mathbf{r} \in \mathbb{F}_2^n \mid (1 + r_i) \left(1 + \sum_{j=1}^n \gamma_{i,j} r_j \right) = 0 \right\}. \tag{13}$$

Note that \mathcal{V} contains the affine subspace

$$\mathcal{A} = \left\{ \mathbf{r} \in \mathbb{F}_2^n \mid \forall i \in \{1, \dots, n\} : \sum_{j=1}^n \gamma_{i,j} r_j = 1 \right\} \tag{14}$$

of the color assignments with the property ‘every vertex has an odd number of black neighbors’. For a large class of graphs, we can make the lower bound $A_n \geq |\mathcal{A}|$ explicit:

Corollary 2 (lower bound on the full-body SL of certain graph states). *Let Γ be a graph that admits a color assignment with the property ‘every vertex has an odd number of black neighbors’. Then, the full-body SL of the corresponding graph state $|\Gamma\rangle$ can be lower bounded as $A_n \geq 2^{\dim(\ker(\Gamma))}$, where $\ker(\Gamma)$ is the null space of the adjacency matrix Γ .*

Proof. Let $\mathbf{r} \in \mathbb{F}_2^n$ be the color assignment with the property $\Gamma \mathbf{r} = \mathbf{1} = (1, \dots, 1)$. Then, each of the $2^{\dim(\ker(\Gamma))}$ vectors of the form $\mathbf{r} + \mathbf{s}$ with $\mathbf{s} \in \ker(\Gamma)$ has the same property, $\Gamma(\mathbf{r} + \mathbf{s}) = \mathbf{1}$, and therefore contributes to A_n . \square

2.2. Formulae for mean and variance of normalized SLDs

For a pure n -qubit state $|\psi\rangle$ the normalized SLD $\mathbf{a} = \mathbf{A}/2^n$ can be regarded as a probability distribution over the set $\{0, \dots, n\}$. In the special case where $|\psi\rangle$ is a stabilizer state with stabilizer group \mathcal{S} , the SLD coincides with the Pauli-weight distribution (PWD) for \mathcal{S} , i.e. a_k is the probability that an operator $S \in \mathcal{S}$ (drawn uniformly at random) has Pauli weight k . Information about the PWD is relevant in the context of simultaneous measurements of all operators in \mathcal{S} [19]. It is possible to infer mean and variance of \mathbf{a} from A_1 and A_2 alone by exploiting the MacWilliams identities

$$\sum_{k=0}^m \binom{n-k}{n-m} A_k = 4^m \sum_{k=0}^n \binom{n-k}{m} \frac{A_k}{2^n}, \tag{15}$$

which hold for all $m \in \{0, \dots, n\}$ and for all pure n -qubit states [1, 11, 12, 20, 21]. Inserting $m = 1$ into equation (15) yields the first moment of the normalized SLD,

$$\langle k \rangle_{\mathbf{a}} = \sum_{k=0}^n k a_k = \frac{3n - A_1}{4}, \tag{16}$$

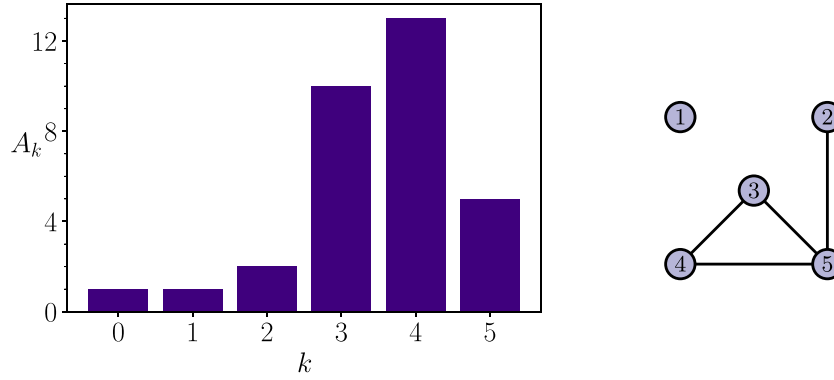


Figure 1. Example of the SLD (left) for a graph state (right) with $n = 5$ vertices and $I = L = T = 1$. Here, vertex 1 is an isolated vertex, while vertex 2 is a leaf. Vertices 3 and 4 form a twin pair because they share the same neighborhood; this fact would not change if the edge between them was removed. By corollary 3, the mean of the normalized SLD \mathbf{a} is given by $\langle k \rangle_{\mathbf{a}} = 7/2$ and its variance is given by $\langle k^2 \rangle_{\mathbf{a}} - \langle k \rangle_{\mathbf{a}}^2 = 5/4$.

and inserting $m = 2$ yields the second moment,

$$\langle k^2 \rangle_{\mathbf{a}} = \sum_{k=0}^n k^2 a_k = \frac{9n^2 + 3n - (6n - 2)A_1 + 2A_2}{16}. \tag{17}$$

Similarly, it is possible to express $\langle k^j \rangle_{\mathbf{a}}$ in terms of A_1, \dots, A_j for all $j \leq n$. By combining equations (16) and (17), we obtain the variance of the normalized SLD,

$$\langle k^2 \rangle_{\mathbf{a}} - \langle k \rangle_{\mathbf{a}}^2 = \frac{3n - (A_1 - 2)A_1 + 2A_2}{16}. \tag{18}$$

Using the bounds $0 \leq A_1 \leq n$ and $0 \leq A_2 \leq \binom{n}{2}$ from [12], we can infer from equations (16)–(18) that all pure states obey $\langle k \rangle_{\mathbf{a}} \in [\frac{n}{2}, \frac{3n}{4}]$, $\langle k^2 \rangle_{\mathbf{a}} \in [\frac{3n^2+5n}{16}, \frac{10n^2+2n}{16}]$, and $\langle k^2 \rangle_{\mathbf{a}} - \langle k \rangle_{\mathbf{a}}^2 \leq \frac{(n+1)^2}{16}$. Here, the minimum mean $\langle k \rangle_{\mathbf{a}} = \frac{n}{2}$ is attained iff $|\psi\rangle$ is fully separable because $A_1 = n$ is equivalent to all 1-body marginals being pure [12]. Combining equations (9) and (16), yields that the maximum mean $\langle k \rangle_{\mathbf{a}} = \frac{3n}{4}$ is reached for all graph states without any isolated vertices and, more generally, for all genuinely multipartite entangled (GME) stabilizer states [5]. Note that equations (16)–(18) do not generalize to states that are not pure, e.g. the maximally mixed state $\rho = \mathbb{1}/2^n$ has $A_1 = A_2 = 0$ but $\langle k \rangle_{\mathbf{a}} = \langle k^2 \rangle_{\mathbf{a}} = 0$.

To compute the mean and variance of the normalized SLD for an arbitrary stabilizer state $|\psi\rangle$, one can efficiently compute a graph state $|\Gamma\rangle$ that is LU-equivalent to $|\psi\rangle$ by exploiting theorem 1 of [16]. Then, one can read off $I, L,$ and T from Γ and exploit equations (9)–(18), see figure 1 for an example. This shows:

Corollary 3 (mean and variance of the normalized SLD of a graph state). *Let Γ be a graph with n vertices, I isolated vertices, L leaves, and T twin pairs. Then, the mean of the normalized SLD \mathbf{a} of $|\Gamma\rangle$ is given by $\langle k \rangle_{\mathbf{a}} = (3n - I)/4$. Furthermore, its variance is given by $\langle k^2 \rangle_{\mathbf{a}} - \langle k \rangle_{\mathbf{a}}^2 = (3n - (I - 2)I + 2(L + T))/16$.*

2.3. Analytical SLDs of various families of graph states

The graph color assignment problem, as formulated in theorem 1, constitutes a powerful tool for understanding the geometry of quantum states. In this section, we introduce families of graph states with certain symmetry properties which allow us to derive analytical formulas of their SLDs.

The *complete graph* K_n has n vertices and each pair of vertices is connected by an edge, i.e. all off-diagonal entries of its adjacency matrix are equal to 1. Its complement $\overline{K_n}$ is appropriately called the *edgeless graph* and the corresponding graph state $|\overline{K_n}\rangle = |+\rangle^{\otimes n}$ is fully separable. For every color assignment of $\overline{K_n}$ it is vacuously true that every white vertex has zero black neighbors. Thus, the graph-theoretical problem from theorem 1 can be simplified as follows. For each $k \in \{0, \dots, n\}$, $A_k^{\text{sep}(n)}$ is equal to the number of color assignments with exactly $n - k$ white vertices. This immediately yields the well-known [6] SLD $A_k^{\text{sep}(n)} = \binom{n}{k}$ of a fully separable, pure n -qubit state.

The *star graph* $K_{1,n-1}$ arises from K_n via local complementation [15] at one of the vertices, say vertex 1. Vertex 1 is then connected to all other vertices via an edge and there are no further edges. Both $|K_n\rangle$ and $|K_{1,n-1}\rangle$ are LU-equivalent to the Greenberger–Horne–Zeilinger state $|\text{GHZ}(n)\rangle = \frac{1}{\sqrt{2}}(|0\rangle^{\otimes n} + |1\rangle^{\otimes n})$ [22]. Let us rederive its well-known [6] SLD

$$A_k^{\text{GHZ}(n)} = \binom{n}{k} \delta_{k,\text{even}} + 2^{n-1} \delta_{k,n}, \tag{19}$$

where $\delta_{k,\text{even}} = \frac{1+(-1)^k}{2}$, by applying theorem 1 to the star graph. If vertex 1 (the central vertex) is black, there are no white vertices with an even number of black neighbors. Thus, all of the 2^{n-1} color assignments $\mathbf{r} \in \mathbb{F}_2^n$ with $r_1 = 1$ contribute to A_n . Now assume that vertex 1 is white. Then, all other vertices have zero black neighbors, which is even. There are $\binom{n-1}{k}$ color assignments for which exactly k of the vertices $2, \dots, n$ are black. If k is even, vertex 1 also has an even number of black neighbors, i.e. such a color assignment contributes to A_k (because $n - k$ vertices are white and all of them have an even number of black neighbors). If k is odd, however, the color assignment contributes to A_{k+1} as only the $n - k - 1$ white vertices with index $i \in \{2, \dots, n\}$ have an even number of black neighbors. Therefore, the SLD of the star graph state is given by $A_k = \binom{n-1}{k-1} + \binom{n-1}{k} = \binom{n}{k}$ if $k < n$ is even, $A_k = 0$ if $k < n$ is odd, and $A_n = 2^{n-1} + \delta_{n,\text{even}}$. This proves equation (19).

The *Pusteblyme graph* [23] is a close cousin of $K_{1,n-1}$, see figure 2. It has $n \geq 5$ vertices and $n - 1$ edges. Vertex 1 has three neighbors: 2, 3, and 4. Vertex 2 has $n - 3$ neighbors: 1, 5, 6, \dots , n . An elementary but lengthy analysis, which we provide in appendix A, shows that the SLD of the n -qubit Pusteblyme graph state, $|\text{Pust}(n)\rangle$, is given by

$$A_k^{\text{Pust}(n)} = \left(\binom{n-3}{k-3} + 3 \binom{n-2}{k-2} + \binom{n-3}{k} \right) \delta_{k,\text{even}} + 3 \times 2^{n-4} \delta_{k,n-2} + 5 \times 2^{n-4} \delta_{k,n}, \tag{20}$$

where we set $\binom{n}{k} = 0$ if n or k is a negative integer. In figure 3, we plot the normalized SLD $\mathbf{a} = \mathbf{A}/2^n$ for a GHZ state (blue) and for a Pusteblyme graph state (yellow). The two distributions have a significant amount of overlap (lavender), which we attribute to the similarity between star graphs and Pusteblyme graphs. In both cases, we observe $a_k = 0$ for all odd k , a property that a graph state exhibits iff all of its vertices have an odd number of neighbors [20, 23]. It is well known that a_n is maximized by the GHZ state, i.e. $a_n^{\text{GHZ}(n)} \geq a_n[\rho]$ for every n -qubit state ρ [9, 11]. In figure 3, we can see that the process of moving two leaves from the central vertex to one of the other leaves (a process which turns $|K_{1,n-1}\rangle$ into $|\text{Pust}(n)\rangle$) has the effect that $a_n^{\text{GHZ}(n)} \approx 0.5$ splits into $a_n^{\text{Pust}(n)} \approx 0.31$ and $a_{n-2}^{\text{Pust}(n)} \approx 0.19$. Since, by corollary 3,

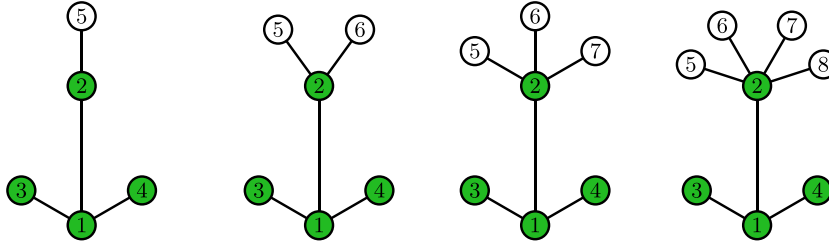


Figure 2. Pustelblume (German for dandelion) graphs with $n \in \{5, 6, 7, 8\}$ vertices.

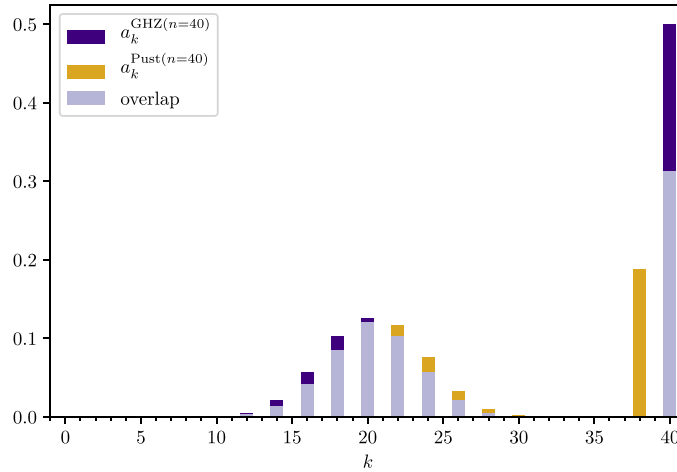


Figure 3. Normalized SLDs $a_k = 2^{-n} A_k$ of $|\text{GHZ}(n)\rangle$ and $|\text{Pust}(n)\rangle$ for $n = 40$ qubits.

both distributions have the same mean, $\langle k \rangle_a = 3n/4$, this splitting of a_n must be compensated somehow. Here, this compensation is ensured by $a_k^{\text{GHZ}(n)} < a_k^{\text{Pust}(n)}$ for $n/2 < k < n$, whereas $a_k^{\text{GHZ}(n)} > a_k^{\text{Pust}(n)}$ for $k \leq n/2$. This explains why the yellow bars in figure 3 are enclosed from both sides by blue bars.

The cycle graph C_n has n vertices, where vertex $i \in \{1, \dots, n\}$ is connected to vertices $i - 1 \pmod n$ and $i + 1 \pmod n$, see figure 4. The corresponding cycle graph state, $|C_n\rangle = |\text{RC}(n)\rangle$, is also known as the ring cluster (RC) state [24], which is a prototypical resource state for measurement-based quantum computation (MBQC) [25, 26]. By exploiting periodic boundary conditions of C_n , we show in appendix B its SLD is given by $A_0^{\text{RC}(n)} = 1$ and

$$A_k^{\text{RC}(n)} = \frac{n}{k} \binom{k}{n-k} + \sum_{m=1}^{\lfloor \frac{k-1}{2} \rfloor} \frac{n}{m} \binom{k-2m-1}{m-1} \sum_{l=0}^{n-k} \binom{k-3m}{n-k-l} \binom{l+m-1}{l} \quad (21)$$

for all $n \geq 3$ and all $k \in \{1, \dots, n\}$. Note that $A_n^{\text{RC}(n)}$ is minimal among all n -qubit graph states with a connected graph of $n \leq 8$ vertices [27]; for $n = 9$, however, there is already a graph state with an even lower n -body SL [28]. As we portray in figure 5 for the example of $n = 100$ qubits, the normalized SLD $\mathbf{a}^{\text{RC}(n)}$ (blue) has a very large overlap (lavender) with the asymmetrical binomial distribution $\mathbf{b}(p)$ for success probability $p = 3/4$ (yellow). By applying corollary 3,

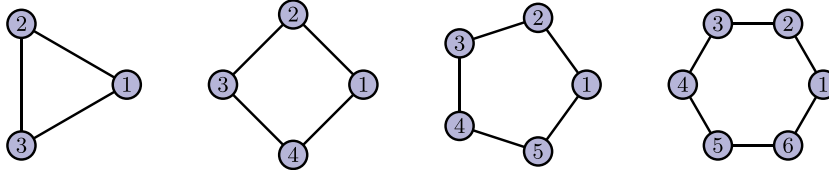


Figure 4. Cycle graphs C_n with $n \in \{3, 4, 5, 6\}$ vertices.

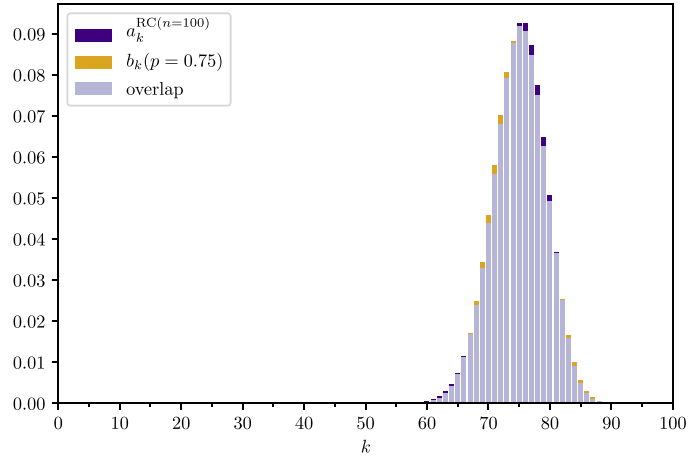


Figure 5. Comparison of the normalized SLD $a_k^{\text{RC}(n)} = 2^{-n} A_k^{\text{RC}(n)}$ of the ring cluster state from equation (21) to an asymmetric binomial distribution $b_k(p = 3/4) = \binom{n}{k} 3^k 4^{-n}$ for $n = 100$.

we find that the mean $\langle k \rangle = 3n/4$ and the variance $\langle k^2 \rangle - \langle k \rangle^2 = 3n/16$ coincide for both distributions. Still, there are minor differences between them: At the left tail, $k \in \{0, \dots, 66\}$, the normalized SLD of the RC state dominates, with the exception of $a_1^{\text{RC}(100)} = a_2^{\text{RC}(100)} = 0$. At the right tail, $k \in \{82, \dots, 100\}$, the binomial distribution takes larger values. Around the peak, the behavior is reversed: The binomial distribution dominates left of the peak, $k \in \{67, \dots, 74\}$, whereas the SLD of the RC state is larger for $k \in \{75, \dots, 81\}$. These minor differences have profound implications on the robustness of the entanglement in $|\text{RC}(n)\rangle$, see section 5.2 and appendix C.

3. Numerical investigation of SLDs of graph states

In the previous section (see figure 5), we noticed how the normalized SLD $\mathbf{a} = (a_0, \dots, a_n)$ of an n -qubit RC state visually matches a binomial distribution $\mathbf{b}(p = 0.75)$, where $b_k(p) = \binom{n}{k} p^k (1-p)^{n-k}$. In this section, we turn such qualitative statements into quantitative ones by investigating the difference of the distributions in terms of the total variation distance

$$\text{TVD}(\mathbf{a}, \mathbf{b}(p)) = \frac{1}{2} \sum_{k=0}^n |a_k - b_k(p)| \in [0, 1]. \tag{22}$$

The TVD is equal to 0 iff the two probability distributions coincide, and equal to 1 iff the supports of \mathbf{a} and $\mathbf{b}(p)$ are disjoint.

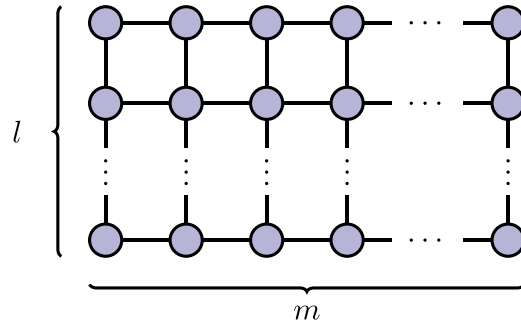


Figure 6. Graph of a 2D cluster state $|C(l, m)\rangle$ with $n = l \times m$ qubits.

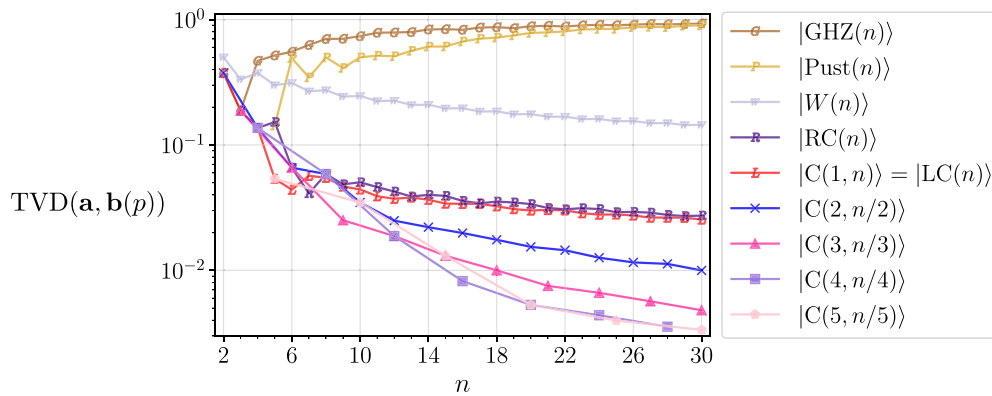


Figure 7. Total variation distance, see equation (22), between the normalized SLD \mathbf{a} of various families of n -qubit states and a corresponding binomial distribution $\mathbf{b}(p)$ with success probability $p = 3/4$ for all states with the exception of $|W(n)\rangle$, where we instead use $p = 1/2$ for reasons explained in appendix D.

3.1. SLDs of cluster states

An important family of well-studied graph states are *cluster states*, which are crucial resource states for MBQC [25, 26]. For example, the 2D cluster state $|C(l, m)\rangle$ has an $l \times m$ grid as its graph, see figure 6. To contribute to the theoretical understanding of cluster states, we now investigate their SLDs as this provides new insights about their stabilizer groups. Furthermore, when applied to corollary 5 in section 5.2, this will yield insights into the noise robustness of the entanglement that is exhibited by these states.

In figure 7, we plot the TVD between the normalized SLD \mathbf{a} of certain n -qubit states and the binomial distribution $\mathbf{b}(p)$ for an appropriately chosen probability p . For the W state (lavender W 's), we choose $p = 0.5$ as this causes $\text{TVD}(\mathbf{a}^{W(n)}, \mathbf{b}(p = 0.5)) \rightarrow 0$ for $n \rightarrow \infty$; for readers that are interested in the important case of SLDs of non-stabilizer states, we provide more details in appendix D. For all other states, we use $p = 0.75$ as this ensures that \mathbf{a} and $\mathbf{b}(p)$ have the same mean, recall corollary 3. We observe in figure 7 that the TVD converges to 1 for GHZ states (brown G 's) and Pusteblyme graph states (yellow P 's). This is because their normalized SLDs are far from being binomial distributions, recall figure 3. As expected, the TVD for RC states (blue R 's) is smaller than for GHZ states and Pusteblyme graph states. With equation (21) at hand (the solution of the graph-theoretical problem for cycle graphs),

we compute $\text{TVD}(\mathbf{a}^{\text{RC}(n)}, \mathbf{b}(p = 0.75))$ for all $n \leq 1000$ and find that $0.15/\sqrt{n}$ fits the data very well for large n .

For the broader class of general cluster states (red to blue), we lack the solution of the graph-theoretical problem, thus, we are limited to $n \leq 30$. Aside from finite size effects, we can see that the TVDs decrease with n . Hereby, the TVD is smaller for 2D cluster states $|\text{C}(l, m)\rangle$ than for $|\text{RC}(n)\rangle$ and 1D linear cluster (LC) states $|\text{LC}(n)\rangle = |\text{C}(1, n)\rangle$ (red L 's). For 2D cluster states, the TVD tends to be smaller for broader cluster patches, e.g. for $n = 30$ qubits, the TVD of the width-2 cluster state (blue crosses) is three times as large as that of the width-5 cluster state (pink pentagons). We also compute the SLD of an analogously-defined 3D cluster state $|\text{C}(3, 3, 3)\rangle$ for $n = 27$ qubits and find an even smaller TVD of 0.00138 (not plotted)⁵.

In conclusion, the normalized SLD is very similar to a binomial distribution for some graph states (cluster states), while for others (GHZ, Pustoblume) it is not. To identify which of the two is the exception and which is the norm, we will next investigate random graph states.

3.2. SLDs of random graph states

To further solidify our understanding of the geometry of quantum states, we now illustrate the behavior of random graphs states. To this end, we employ the Erdős–Rényi graph model [29], however, we expect that similar results hold true for other common random graph models as well. Given a probability $q \in [0, 1]$, a random Erdős–Rényi graph with n vertices is created as follows: for each $i \in \{1, \dots, n\}$ and $j \in \{i + 1, \dots, n\}$, an edge between vertex i and j is created with probability q . We denote the resulting random variable as $\Gamma_n^{(q)}$. The probability of drawing a specific graph $\Gamma \sim \Gamma_n^{(q)}$ only depends on its number of edges $e(\Gamma)$ and is given by

$$\Pr[\Gamma_n^{(q)} = \Gamma] = q^{e(\Gamma)}(1 - q)^{\binom{n}{2} - e(\Gamma)}. \tag{23}$$

In particular, $\langle A_1 \rangle_q = n(1 - q)^{n-1}$ is the expected number of isolated vertices. Thus, by corollary 3, the expected mean of the SLD of a random graph state is given by

$$\langle \langle k \rangle_{\mathbf{a}} \rangle_q = \frac{3n}{4} - \frac{n(1 - q)^{n-1}}{4}, \tag{24}$$

which is approximately equal to $3n/4$ if q and n are large enough.

In a numerical experiment, we sample Erdős–Rényi graphs with $n \in \{5, 10, 15, 20\}$ vertices and compute the normalized SLD \mathbf{a} of the corresponding random graph states. Then, we calculate the TVD between \mathbf{a} and a binomial distribution $\mathbf{b}(p)$ with the same mean, i.e. for each sample holds $\langle k \rangle_{\mathbf{a}} = np$. In figure 8, we plot the result over the whole interval $q \in [0, 1]$ with a step size of 0.01. For complexity reasons, we vary the number of samples from 10^5 for $n = 5$ (blue) to 10^2 for $n = 20$ (brown). Overall, the curves show a similar behavior albeit less pronounced for $n = 5$ due to finite size effects. For $q = 0$, there are no edges and every sampled graph state is equal to $|\Gamma\rangle = |+\rangle^{\otimes n}$. Since the normalized SLD of such a fully separable state is equal to a symmetric binomial distribution, the TVD between the two distributions vanishes. As $q \gtrsim 0$ grows, the TVD first begins to increase before it drops again and stagnates at a very small value over a wide range of q . The latter observation implies that random graph states with $\langle \text{TVD}(\mathbf{a}, \mathbf{b}(p)) \rangle_q \approx 0$ are abundant. We attribute the small initial peak at small $q > 0$ to the

⁵ Digital feature: For the graph of $|\text{C}(3, 3, 3)\rangle$ and its SLD, please click on this [link](#).

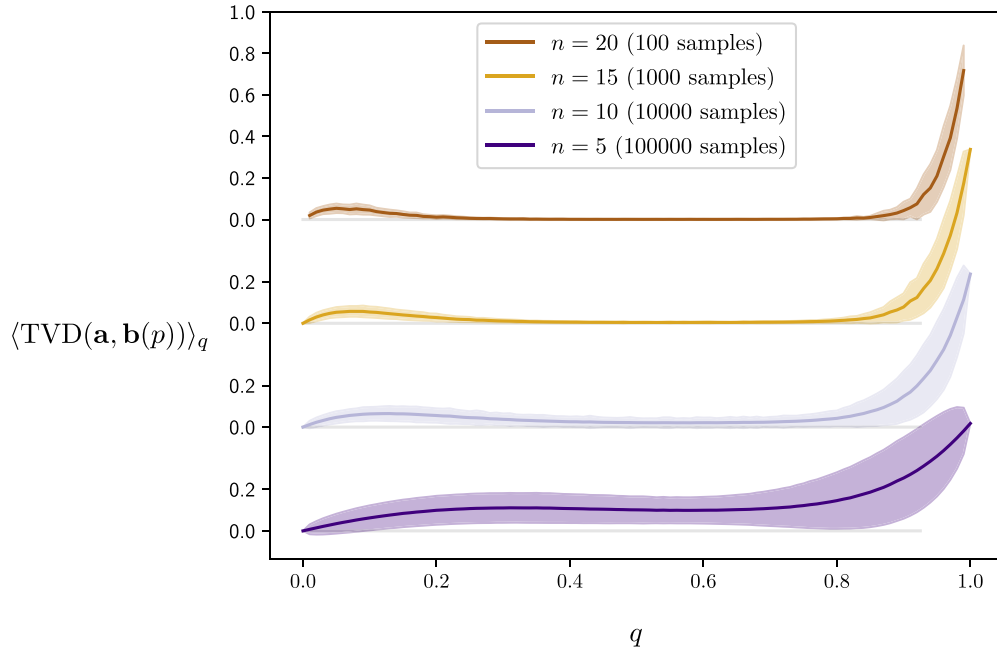


Figure 8. Total variation distance, see equation (22), between the normalized SLD \mathbf{a} of random graph states and a corresponding binomial distribution $\mathbf{b}(p)$, where p is selected for every individual graph such that the two distributions have the same mean. In the generation of the random graphs, an edge between each pair of qubits is created with probability q . The shaded region marks the range in which the TVD lies with probability 68% (1 sigma). For better readability, the curves have an offset spacing.

existence of tensor factors that are LU-equivalent to $|\text{GHZ}(m)\rangle$ for small values of $m < n$.⁶ The position of the peak is consistent with $q \approx \ln(n)/n$, which is the threshold below (above) which $\Gamma \sim \Gamma_n^{(q)}$ is almost surely disconnected (connected) [29]. Around $q \approx 0.8$ the TVD suddenly starts to grow again and eventually, at $q = 1$, the complete graph is reached and $|\Gamma\rangle = |K_n\rangle$ is LU-equivalent to $|\text{GHZ}(n)\rangle$, which has a very large TVD to the corresponding binomial distributions; recall figure 7. For larger n , we observe a decline of TVD at intermediate values of q , e.g. at $q = 0.5$ we find the values $\langle \langle k \rangle_{\mathbf{a}} \rangle_q = 0.10(6)$ for $n = 5$, $\langle \langle k \rangle_{\mathbf{a}} \rangle_q = 0.02(2)$ for $n = 10$, $\langle \langle k \rangle_{\mathbf{a}} \rangle_q = 0.004(3)$ for $n = 15$, and $\langle \langle k \rangle_{\mathbf{a}} \rangle_q = 0.0007(4)$ for $n = 20$. Also, the plateau of small TVD values is broader for larger n as both the small initial peak and the final steep are sharpened.

To explain the emergence of the plateaus in figure 8, we show in appendix E that the expected k -body SL of an n -vertex Erdős–Rényi graph state with edge-probability q is given by

$$\langle A_k \rangle_q = \binom{n}{k} 2^{-n} \sum_{b=0}^k \binom{k}{b} 2^b (1 + (1 - 2q)^b)^{n-k} (1 - (1 - 2q)^b)^{k-b}. \quad (25)$$

⁶ If the edge probability q is small, there will be many graph components with a small number m of vertices. For $m = 2$ and $m = 3$, every graph state is LU-equivalent to a GHZ state, and for $m = 4$, GHZ and cycle graph are the only LU equivalence classes. The SLDs of GHZ states are far from the binomial distribution, see figure 7. This (total variational) distance is inherited by SLDs of product states that contain a considerable amount of GHZ states.

For $n \gg 1$, we can use the approximation $\binom{k}{b} 2^b (1 + (1 - 2q)^b)^{n-k} (1 - (1 - 2q)^b)^{k-b} \approx \binom{k}{b} 2^b$ at a wide range around $q \approx 1/2$. This allows us to simplify equation (25) using the binomial theorem, which yields

$$\langle a_k \rangle_q \approx \binom{n}{k} 4^{-n} \sum_{b=0}^k \binom{k}{b} 2^b = \binom{n}{k} 3^k 4^{-n} = B_k(p = 3/4). \tag{26}$$

The plateaus in figure 8 show for which values of n and q the approximation in equation (26) is valid.

A direct physical consequence of the results in figure 8 is the following: if we prepare the state $|+\rangle^{\otimes n}$, where $n \gg 5$, and apply to each pair of qubits a controlled-Z gate with probability $0 \ll q \ll 1$ (and do nothing with probability $1 - q$), then we should expect that the SLD of the resulting state is approximately given by $A_k \approx \binom{n}{k} 3^k 2^{-n}$. However, this approximation should be applied with care, see footnote 7 in appendix C for an example of what can go wrong otherwise.

Now, we are finally in the position to answer the question raised at the end of section 3.1: there is an abundance of random graph states for which the normalized SLD is remarkably close to an asymmetrical binomial distribution; we call SLDs with this property *generic*. In that sense, cluster graphs have generic SLDs (recall figure 5), whereas star, complete, and Pustebume graphs do not (recall figure 3). Hence, we will say that SLDs of the latter graph states are *special*. Also note that among the 4^n Pauli operators of the form $X^r Z^s$, there are exactly $\binom{n}{k} 3^k$ operators with $\text{wt}(X^r Z^s) = k$. This shows that the PWD of the stabilizer group of a graph state with a generic SLD closely resembles the PWD of the full Pauli group.

4. Generalization to higher-dimensional qudits

In this section, we extend the scope of our investigation to the case of n -qudit states, where every qudit has a Hilbert space dimension of $d \geq 2$. For studying such states, we find it convenient to label the computational basis by elements of the free module $(\mathbb{Z}/d\mathbb{Z})^n$ over the ring $\mathbb{Z}/d\mathbb{Z} = \{0, 1, \dots, d - 1\}$ of integers modulo d . In this way, any pure state can be written as a superposition of states of the form $|j\rangle$, where $j \in (\mathbb{Z}/d\mathbb{Z})^n$. Moreover, a general mixed state for n qudits can be written as

$$\rho = \frac{1}{d^n} \sum_{\mathbf{r}, \mathbf{s} \in (\mathbb{Z}/d\mathbb{Z})^n} \rho_{\mathbf{r}, \mathbf{s}} X_d^{\mathbf{r}} Z_d^{\mathbf{s}} \tag{27}$$

for unique coefficients $\rho_{\mathbf{r}, \mathbf{s}} \in \mathbb{C}$, where the *generalized Pauli operators* can be defined as

$$X_d^{\mathbf{r}} Z_d^{\mathbf{s}} = \sum_{\mathbf{j} \in (\mathbb{Z}/d\mathbb{Z})^n} \omega_d^{\mathbf{j} \cdot \mathbf{s}} |\mathbf{j} + \mathbf{r}\rangle \langle \mathbf{j}| \tag{28}$$

and $\omega_d = \exp(2\pi i/d)$ [30]. Then, the n -qudit k -body SL of ρ is defined as

$$A_k[\rho] = \sum_{\substack{\mathbf{r}, \mathbf{s} \in (\mathbb{Z}/d\mathbb{Z})^n \\ \text{swt}_d(\mathbf{r}, \mathbf{s}) = k}} |\text{Tr}[\rho X_d^{\mathbf{r}} Z_d^{\mathbf{s}}]|^2 = \sum_{\substack{\mathbf{r}, \mathbf{s} \in (\mathbb{Z}/d\mathbb{Z})^n \\ \text{swt}_d(\mathbf{r}, \mathbf{s}) = k}} |\rho_{\mathbf{r}, \mathbf{s}}|^2, \tag{29}$$

where $\text{swt}_d(\mathbf{r}, \mathbf{s}) = |\{i \in \{1, \dots, n\} \mid r_i \neq 0 \vee s_i \neq 0\}|$ is the symplectic weight for qudits [11]. Note the similarity between equations (3) and (29). If ρ is a pure state, the normalized SLD $\mathbf{a} = \mathbf{A}/d^n$ is a probability distribution, and equation (15) generalizes to

$$\sum_{k=0}^m \binom{n-k}{m-k} A_k = d^{2m} \sum_{k=0}^n \binom{n-k}{m} a_k \tag{30}$$

for all $m \in \{0, \dots, n\}$ [11, 12, 21]. After inserting $m = 1$ and $m = 2$ into equation (30), and after a little algebra, we find

$$\langle k \rangle_{\mathbf{a}} = \frac{(d^2 - 1)n - A_1}{d^2} \tag{31}$$

$$\text{and } \langle k^2 \rangle_{\mathbf{a}} = \frac{d^4 n^2 - d^2(2n - 1)n + n(n - 1) + (2(n - 1) - d^2(2n - 1))A_1 + 2A_2}{d^4}. \tag{32}$$

Note that equations (31) and (32) generalize equations (16) and (17) to the case of pure n -qudit states; to the best of our knowledge, both results are new.

4.1. Known results about SLDs of qudit states

For every Abelian subgroup $\mathcal{S} \subset \mathcal{P}_d^n$ of the n -qudit Pauli group

$$\mathcal{P}_d^n = \{ \omega_{2d}^q X^{\mathbf{r}} Z^{\mathbf{s}} \mid q \in \mathbb{Z}/2d\mathbb{Z}, \mathbf{r}, \mathbf{s} \in (\mathbb{Z}/d\mathbb{Z})^n \} \tag{33}$$

with $|\mathcal{S}| = d^n$ and $z\mathbb{1} \notin \mathcal{S}$ for $z \in \mathbb{C} \setminus \{1\}$, there exists a unique *stabilizer state* $|\psi\rangle \in (\mathbb{C}^d)^{\otimes n}$ which, by definition, fulfills $S|\psi\rangle = |\psi\rangle$ for all $S \in \mathcal{S}$ [2, 31]. In this case, the k -body SL is equal to the number of *stabilizer operators* $S \in \mathcal{S}$ which have a Pauli weight of k [8]. For example, the n -qudit GHZ state

$$|\text{GHZ}_d(n)\rangle = \frac{1}{\sqrt{d}} (|0\rangle^{\otimes n} + \dots + |d-1\rangle^{\otimes n}) \tag{34}$$

is a stabilizer state for which \mathcal{S} is generated by $X_d \otimes \dots \otimes X_d$ and $Z_d^{(i)} Z_d^{(i+1)\dagger}$ for all $i \in \{1, \dots, n-1\}$. In proposition 10 of [27], we have derived its SLD

$$A_k^{\text{GHZ}_d(n)} = \binom{n}{k} \frac{(d-1)^k + (-1)^k (d-1)}{d} + \delta_{k,n} (d-1) d^{n-1} \tag{35}$$

by counting all weight- k operators in \mathcal{S} (see [11] for an alternative proof). For every symmetric matrix $\Gamma = (\gamma_{i,j}) \in (\mathbb{Z}/d\mathbb{Z})^{n \times n}$ with zeros on the diagonal, a *qudit graph state*

$$|\Gamma\rangle = \frac{1}{\sqrt{d^n}} \sum_{\mathbf{r} \in (\mathbb{Z}/d\mathbb{Z})^n} \omega_d^{\sum_{i=1}^n \sum_{j=i+1}^n r_i \gamma_{i,j} r_j} |\mathbf{r}\rangle \tag{36}$$

is defined [32–34]. An important example is $|+_d\rangle^{\otimes n} = \frac{1}{\sqrt{d^n}} \sum_{\mathbf{k} \in (\mathbb{Z}/d\mathbb{Z})^n} |\mathbf{k}\rangle$, which is the graph state with the trivial adjacency matrix $\Gamma = 0$. As the stabilizer group of $|+_d\rangle^{\otimes n}$ is given by $\mathcal{S} = \{X_d^{\mathbf{r}} \mid \mathbf{r} \in (\mathbb{Z}/d\mathbb{Z})^n\}$, its SLD follows as $A_k^{\text{sep}_d(n)} = \binom{n}{k} (d-1)^k$.

Since SLs are convex and LU-invariant, the k -body SL of a fully separable state cannot exceed $A_k^{\text{sep}_d(n)}$. In other words, every n -qudit state with

$$A_k[\rho] > \binom{n}{k} (d-1)^k \tag{37}$$

is entangled [9, 10]. We refer to equation (37) as the *k -body SL criterion*. In all examples we know of, the n -body SL criterion is stronger than other k -body SL criteria. To experimentally verify that a state ρ is entangled, it is therefore sufficient to measure the expectation values $\text{Tr}[\rho P_i]$ for an increasing number N of weight- n Pauli operators $P_1, \dots, P_N \in \mathcal{P}_d^n$ until $\sum_{i=1}^N |\text{Tr}[\rho P_i]|^2$ exceeds the full-separability bound $(d-1)^n$ with high confidence. This

approach is particularly promising for qubits, where estimating only $N = 2$ Pauli expectation values can be sufficient. For $D > 2$, on the other hand, this entanglement test is not scalable as an exponential (in n) number of Pauli expectation values would need to be estimated experimentally. Note that for every ideal, i.e. noise-free, graph state $|\Gamma\rangle$, the n -body SL is lower bounded as

$$A_n[|\Gamma\rangle\langle\Gamma|] \geq A_n^{\text{sep}_d(n)} = (d - 1)^n \tag{38}$$

because (up to a global phase) $X^{\mathbf{r}}Z^{\Gamma\mathbf{r}}$ is a weight- n stabilizer operator of $|\Gamma\rangle$ for every $\mathbf{r} \in \{1, \dots, d - 1\}^n$. For a technical discussion how the bound in equation (38) can be improved, see appendix B in [27]. It is well known that in the case of qubits, A_n is maximized by the GHZ state, but for higher-dimensional qudits, A_n is maximized by a biseparable state [9, 11]. Furthermore, some GME states with $A_n = 0$ have been identified [35]. These two facts demonstrate that A_n only contains limited information about the entanglement of a state. If the SLD is considered as a whole, however, it is possible to establish that a state is GME in a few cases [7]. For these reasons, here we will also adopt the mindset that the SLD should be considered as a whole.

4.2. A novel entanglement criterion for multi-qudit states based on SLDs

By exploiting the purity criterion [5], we can derive the following entanglement criterion.

Theorem 4 (purity criterion applied to SLDs). *Let $\mathbf{A} = (A_0, \dots, A_n)$ be the SLD of an n -qudit state, ρ , with qudit dimension $d \geq 2$. If*

$$\sum_{k=0}^n ((d - 1)n - dk) A_k[\rho] < 0, \tag{39}$$

then ρ is entangled.

The proof of a generalized version of this theorem is stated in appendix G. To apply theorem 4, the only information needed about a state is its SLD. In the special case where $|\Gamma\rangle$ is an n -qudit graph state, we can relate the SLD to a graph-theoretical problem that generalizes theorem 1. For this, we associate every element $r \in \mathbb{Z}/d\mathbb{Z}$ with a color. Then, each color assignment (with d colors) of Γ corresponds to a stabilizer operator $X^{\mathbf{r}}Z^{\Gamma\mathbf{r}}$ (up to phase) and contributes to A_k iff exactly $n - k$ white ($r_i = 0$) vertices $i \in \{1, \dots, n\}$ have the property

$$\sum_{j=1}^n \gamma_{i,j} r_j = 0. \tag{40}$$

Only for qubits, equation (40) simplifies to the property ‘the number of vertices j with $\gamma_{i,j} = 1$ and $r_j = 1$ is equal to 0 modulo 2, i.e. even’. In the qudit case, the situation is more involved. This is because computing A_k amounts to counting solutions to equations in modular arithmetic, see appendix F for a more detailed treatment. Here, we restrict ourselves to presenting only some of our less-technical results: If d is a prime number, we find

$$A_1 = (d - 1)I \tag{41}$$

as a generalization of equation (9), where I again denotes the number of isolated vertices of Γ . Furthermore, we find for d prime that the 2-body SL obeys

$$T_0(d - 1)^2 + (L + T_1)(d - 1) \leq A_2 \leq T_0(d - 1)^2 + \left(L + \sum_{m=1}^{n-2} T_m \right) (d - 1), \tag{42}$$

where L is the number of leaves and T_m denotes the number of (twin) vertex pairs with exactly m common neighbors and zero non-shared neighbors, e.g. $T_0 = \binom{L}{2}$. For a given graph state $|\Gamma\rangle$, one can efficiently compute the exact value of A_2 by exploiting the formula

$$A_k = \sum_{b=1}^k \sum_{\mathbf{r} \in \mathcal{D}_b} \delta_{\text{swt}_d(\mathbf{r}, \Gamma \mathbf{r}), k}, \tag{43}$$

which generalizes equation (11) and holds for arbitrary $d \geq 2$ and $k \geq 1$. Here, $\mathcal{D}_b \subset (\mathbb{Z}/d\mathbb{Z})^n$ denotes the subset of ‘dit’ strings with exactly b nonzero entries. The evaluation runtime of equation (43) is given by $\mathcal{O}((dn)^k)$, which is efficient for small values of k . This also enables the efficient computation of the mean and the variance of the normalized SLD of a qudit graph state for arbitrary d via equations (31) and (32). Finally note that, if d is prime, every n -qudit stabilizer state is LU-equivalent to a qudit graph state [33], which further extends the applicability of our results.

5. SLDs of noisy states

Until this point, we have exclusively focused on SLDs of *pure* quantum states. In reality, however, experimental imprecision and decoherence always lead to some uncertainty about the state of a quantum system. This necessitates that we extend our discussion to the more general case of *mixed* states. In section 5.1, we investigate the impact of noise on the SLD of a general n -qudit state. Then, in section 5.2, we apply our insights for the derivation of noise levels below which entanglement is preserved.

5.1. The impact of noise on qudit SLDs

The n -qudit depolarizing channel of strength $p \in [0, 1]$, which is defined via

$$\mathcal{E}_{\text{glob}}^{(p)}[\rho] = (1-p)\rho + p \frac{\mathbb{1}}{d^n}, \tag{44}$$

is a very simplistic model that describes *global white noise* acting on all qudits simultaneously. Since there are only two terms in equation (44), global white noise is easy to treat theoretically and, therefore, often used as a first approximation. A more realistic error channel, which takes spatial separation of qudits into account, is the *local white noise channel*

$$\mathcal{E}_{\text{loc}}^{(p)}[\rho] = \left(\mathcal{E}^{(p)}\right)^{\otimes n} [\rho], \tag{45}$$

where $\mathcal{E}^{(p)}$ denotes the single-qudit depolarizing channel of strength p . Both the global and the local white noise channel are generalized Pauli channels,

$$\mathcal{E}_{\text{glob/loc}}^{(p)}[\rho] = \sum_{\mathbf{r}, \mathbf{s} \in (\mathbb{Z}/d\mathbb{Z})^n} p_{\mathbf{r}, \mathbf{s}}^{\text{glob/loc}} (X_d^{\mathbf{r}} Z_d^{\mathbf{s}}) \rho (X_d^{\mathbf{r}} Z_d^{\mathbf{s}})^\dagger, \tag{46}$$

where a discrete Pauli error $X_d^{\mathbf{r}} Z_d^{\mathbf{s}}$ occurs with probability

$$p_{\mathbf{r}, \mathbf{s}}^{\text{glob}} = \begin{cases} 1-p + \frac{p}{d^{2n}}, & \text{if } \mathbf{r} = \mathbf{s} = (0, \dots, 0) \\ \frac{p}{d^{2n}}, & \text{otherwise} \end{cases} \tag{47}$$

and

$$p_{\mathbf{r}, \mathbf{s}}^{\text{loc}} = \left(\frac{p}{d^2}\right)^{\text{swt}_d(\mathbf{r}, \mathbf{s})} \left(1-p + \frac{p}{d^2}\right)^{n-\text{swt}_d(\mathbf{r}, \mathbf{s})}, \tag{48}$$

respectively [36]. To establish the influence of any given quantum channel \mathcal{E} on the Bloch decomposition of an n -qudit state ρ as in equation (27), it suffices to compute how \mathcal{E} acts on individual Pauli operators. This is because \mathcal{E} is a linear map,

$$\mathcal{E} \left[\frac{1}{d^n} \sum_{\mathbf{r}, \mathbf{s} \in (\mathbb{Z}/d\mathbb{Z})^n} \rho_{\mathbf{r}, \mathbf{s}} X_d^{\mathbf{r}} Z_d^{\mathbf{s}} \right] = \frac{1}{d^n} \sum_{\mathbf{r}, \mathbf{s} \in (\mathbb{Z}/d\mathbb{Z})^n} \rho_{\mathbf{r}, \mathbf{s}} \mathcal{E} [X_d^{\mathbf{r}} Z_d^{\mathbf{s}}]. \quad (49)$$

By exploiting $\text{Tr}[X_d^{\mathbf{r}} Z_d^{\mathbf{s}}] = \delta_{\mathbf{r}, \mathbf{0}} \delta_{\mathbf{s}, \mathbf{0}} d^n$, we find

$$\mathcal{E}_{\text{glob}}^{(p)} [X_d^{\mathbf{r}} Z_d^{\mathbf{s}}] = (1-p) X_d^{\mathbf{r}} Z_d^{\mathbf{s}} + p \text{Tr}[X_d^{\mathbf{r}} Z_d^{\mathbf{s}}] \frac{\mathbb{1}}{d^n} = \begin{cases} \mathbb{1}, & \text{if } \mathbf{r} = \mathbf{s} = \mathbf{0} \\ (1-p) X_d^{\mathbf{r}} Z_d^{\mathbf{s}}, & \text{otherwise} \end{cases} \quad (50)$$

for the global white noise channel and

$$\mathcal{E}_{\text{loc}}^{(p)} [X_d^{\mathbf{r}} Z_d^{\mathbf{s}}] = \bigotimes_{i=1}^n \left((1-p) X_d^{r_i} Z_d^{s_i} + p \text{Tr}[X_d^{r_i} Z_d^{s_i}] \frac{\mathbb{1}}{d} \right) = (1-p)^{\text{swt}_d(\mathbf{r}, \mathbf{s})} X_d^{\mathbf{r}} Z_d^{\mathbf{s}} \quad (51)$$

for local white noise. Inserting this into equation (29) yields the k -body SLs,

$$A_k \left[\mathcal{E}_{\text{glob}}^{(p)} [\rho] \right] = (1-p)^2 A_k [\rho] \quad (52)$$

$$\text{and } A_k \left[\mathcal{E}_{\text{loc}}^{(p)} [\rho] \right] = (1-p)^{2k} A_k [\rho] \quad (53)$$

of the noisy states $\mathcal{E}_{\text{glob}}^{(p)} [\rho]$ and $\mathcal{E}_{\text{loc}}^{(p)} [\rho]$. Since the prefactor $(1-p)^{2k}$ is exponentially suppressed, the correlations between large numbers of subsystems are strongly diminished in the presence of local white noise. This is unsurprising because, by equation (48), Pauli errors $X_d^{\mathbf{r}} Z_d^{\mathbf{s}}$ that jointly affect a large number $k = \text{swt}_d(\mathbf{r}, \mathbf{s})$ of subsystems are very unlikely to occur. In a recent work [37], where equation (53) was independently derived, this insight played a role in establishing stringent limitations on the experimental feasibility of quantum error mitigation protocols on near-term quantum computers.

5.2. Lower bounds on entanglement noise thresholds

Quantum entanglement is a crucial resource for many quantum information protocols, especially in quantum communication [5, 38]. Here, we address the question ‘*how much noise can an entangled state tolerate before it becomes fully separable?*’.

For example, if $|\psi\rangle$ is an n -qudit stabilizer state that is not fully separable, then the noisy state $\mathcal{E}_{\text{glob}}^{(p)} [|\psi\rangle\langle\psi|]$ is also entangled for all values of p that are smaller than

$$p_{\text{PPT, glob}}^{\text{stab}} = 1 - \frac{1}{d^{n-1} + 1}, \quad (54)$$

as we show in [27] for arbitrary d and n by exploiting the positive partial transpose (PPT) criterion [39, 40]. While equation (54) is both simple and general, its physical relevance is questionable since $p_{\text{PPT, glob}}^{\text{stab}} \rightarrow 1$ for $n \rightarrow \infty$. In other words, entanglement can be preserved arbitrarily well by adding more and more qudits in state $|0\rangle$ to a system that is affected by global white noise. This behavior is clearly unphysical in a quantum communication setting, in which the qudits are spatially separated. For this setting, the local white noise model is more appropriate.

Luckily, it is also possible to derive noise thresholds for the case of local white noise, e.g. we can insert equation (53) into equation (37) and solve for p . For every n -qudit state ρ , this yields that the noisy state $\mathcal{E}_{\text{loc}}^{(p)} [\rho]$ is entangled for all values of p below

$$p_{nSL,loc} = 1 - \sqrt[2n]{\frac{(d-1)^n}{A_n[\rho]}}. \tag{55}$$

Recall from equation (38) that every n -qudit graph state $|\Gamma\rangle$ has $A_n \geq (d-1)^n$. Hence, for a nontrivial threshold $p_{nSL,loc} > 0$ it is sufficient that the graph Γ admits a color assignment contributing to A_n with at least one white vertex. Furthermore, we can exploit equation (53) in combination with our new entanglement criterion from theorem 4 to derive the following result:

Corollary 5 (local-white-noise threshold for entanglement). *Let ρ be an n -qudit state that is entangled by theorem 4. Then, the polynomial function*

$$f: [0, 1] \rightarrow \mathbb{R}, \quad p \mapsto \sum_{k=0}^n ((d-1)n - dk) (1-p)^{2k} A_k[\rho] \tag{56}$$

has a root $p_{pur,loc} \in (0, 1)$ at which the sign of f changes from minus to plus. Moreover, every such solution is a lower bound on the local-white-noise threshold for entanglement, i.e. $\mathcal{E}_{loc}^{(p)}[\rho]$ is entangled for every value of $p < p_{pur,loc}$.

Proof. By assumption, we have $f(0) < 0$. Because of $f(1) = (d-1)n > 0$, a solution of $f(p_{pur,loc}) = 0$ with $0 < p_{pur,loc} < 1$ and the desired sign change is guaranteed by the intermediate value theorem. Without loss of generality, $p_{pur,loc}$ is the largest (polynomials have finitely many roots) such solution. Now, let $p < p_{pur,loc}$ and consider the state $\rho' = \mathcal{E}_{loc}^{(p)}[\rho]$. By construction, it is possible to select $p' \in [p, p_{pur,loc})$ with $f(p') < 0$. Because of $0 \leq p \leq p' < 1$, we have $0 \leq \frac{p'-p}{1-p} < 1$. Thus, we can apply a depolarizing channel of strength $q = \frac{p'-p}{1-p}$ to every qudit of ρ' . Because of $\mathcal{E}_{loc}^{(q)}[\mathcal{E}_{loc}^{(p)}[\rho]] = \mathcal{E}_{loc}^{(p+q-pq)}[\rho]$, this results in the state $\mathcal{E}_{loc}^{(q)}[\rho'] = \mathcal{E}_{loc}^{(p')}[\rho]$, which is entangled by $f(p') < 0$. Since local operations cannot create entanglement, the initial state ρ' must have been entangled as well. \square

Note that corollary 5 is constructive as $p_{pur,loc} > 0$ can always be found algorithmically, for instance via the bisection method. For example, we can apply corollary 5 to the logical states $|0\rangle_L, |1\rangle_L, |+\rangle_L$, and $|-\rangle_L$ of the $[[n, 1, \sqrt{n}]]$ rotated surface code [41, 42], all of which have the same SLD $\mathbf{A}^{surf(n)}$ because the logical operators X_L and Z_L are transversal. For the smallest nontrivial instance of the rotated surface code, we find

$$\mathbf{A}^{surf(9)} = (1, 0, 4, 12, 22, 52, 100, 148, 129, 44), \tag{57}$$

which yields $p_{pur,loc}^{surf(9)} \approx 0.28$, whereas the bound $p_{nSL,loc}^{surf(9)} \approx 0.19$ from equation (55), which is based on the previously-known n -body SL criterion, is weaker. Both bounds show that the entanglement-noise threshold for $|0\rangle_L$ etc lies well above the error-correcting threshold $\sim 1\%$ of the surface code [43]. Similarly, we compute

$$\begin{aligned} \mathbf{A}^{surf(25)} = & (1, 0, 8, 0, 72, 80, 534, 984, 3715, 8776, 25816, 62160, 158448, \\ & 386416, 782532, 1561984, 2726047, 3951328, 5115376, 5666352, \\ & 5136632, 3919936, 2437206, 1141160, 390829, 78040), \end{aligned} \tag{58}$$

which yields $p_{pur,loc}^{surf(25)} \approx 0.31$ and $p_{nSL,loc}^{surf(25)} \approx 0.20$. This indicates that entanglement is better preserved in states of QECCs with larger code distances. We find similar results for other families of stabilizer states and refer the interested reader to appendix C.

6. Conclusion and outlook

In this paper, we developed the theory of SLDs of graph states, which has its historical origins in [44, 45]. The starting point of our exploration was theorem 1, which relates SLDs to a graph color assignment problem. By solving this problem in the special case of Pusteblume graph states and RC states, we derived explicit formulas for their SLDs. In this way, we extended the list of analytically known SLDs, which to our knowledge was hitherto limited to fully separable states, GHZ states, Dicke states, and tensor products thereof [6]. For graph states based on random Erdős–Rényi graphs, we discovered that the normalized SLD is remarkably close to an asymmetrical binomial distribution; hence, we proposed to call such SLDs *generic*. This discovery was spurred by a visualization tool that we report separately in [23]. While SLDs of GHZ states and alike are not generic, those of cluster states are. Hence, RC states now constitute the only family of states with analytically-known, generic SLDs. Further consequences of theorem 1 are captured in corollaries 2 and 3, which provide simple formulas for a bound on the full-body SL for certain graph states and for the mean and the variance of the normalized SLD for arbitrary graph states, respectively. Additionally, we formulated similar results for the more general case of higher-dimensional qudits.

While our theoretical developments have their own intrinsic academic relevance, we can also apply them to tackle difficult relevant problems in other branches of quantum information theory. To accomplish this, in theorem 4 we reformulate the purity criterion [46] such that (a potentially weaker form of) it can be tested based on knowledge of the SLD alone. After having derived formulas for the decline of SLDs in the presence of noise, we deduce corollary 5 and apply it to compute lower bounds on noise thresholds for entanglement. In some cases, this approach allows us to outperform the best previous results based on other criteria [47].

By definition, the SLDs are invariants of degree two in the quantum state. Analogous to other hierarchies of entanglement criteria [48], we expect more information on the state to be embodied in higher-degree invariants. Thus, further research could focus on investigating higher-degree generalizations of SLDs. Similarly, it could be fruitful to extend the discussion of qudit graph states to the case of continuous variable systems [49, 50], and search for easily-applicable entanglement criteria that are similar to our theorem 4.

We envision that our graph-theoretical formulation of the SLD problem will facilitate the discovery of SLDs for a wider range of quantum states, e.g. for certain logical states of quantum error-correcting (QEC) codes or for cluster states that appear in MBQC. As QEC and MBQC are fields that heavily rely on the stabilizer formalism, we anticipate that our results will find applications there. Last but not least, we hope that our work will stimulate the investigation of SLDs in a more general setting, e.g. for Dicke states for which the SLDs are available [6], or for qubit (or qudit) hypergraph states for which a theory of SLDs is not developed yet [51].

Data availability statement

The data cannot be made publicly available upon publication because they are not available in a format that is sufficiently accessible or reusable by other researchers. The data that support the findings of this study are available upon reasonable request from the authors.

Acknowledgments

We thank Lennart Bittel, Felix Huber, Matthias Miller, and Gordon Royle for fruitful discussions. This research is part of a project that has received funding from the European

Union’s Horizon 2020 research and innovation programme under the Marie Skłodowska-Curie Grant Agreement No. 847471. This work was supported as a part of NCCR SPIN, a National Centre of Competence (or Excellence) in Research, funded by the Swiss National Science Foundation (Grant Number 51NF40-180604). This work received financial support from the Munich Quantum Valley (K-8), the BMBF (HYBRID, REALISTIQ, MUNIQC-Atoms), and the EU Quantum Technology Flagship (MILLENION). N W acknowledges support by the QuantERA project QuICHE via the German Ministry of Education and Research (BMBF Grant No. 16KIS1119K). IBM, the IBM logo, and ibm.com are trademarks of International Business Machines Corp., registered in many jurisdictions worldwide. Other product and service names might be trademarks of IBM or other companies. The current list of IBM trademarks is available at www.ibm.com/legal/copytrade.

Appendix A. Solution of the graph-theoretical problem for the Pustebume graph

Here we solve the color assignment problem for Pustebume graphs, see figure 2, which will prove equation (20) from the main text. To accomplish this, we distinguish the four cases where vertices 1 and 2 are black and white, respectively. Note that, in each case, there are 2^{n-2} color assignments that contribute to certain SLs.

- If both vertex 1 and 2 are black, see figure 9(a), there cannot be a white vertex with an even number of black neighbors because all remaining vertices are leaves with a black neighbor. Thus, all 2^{n-2} color assignments of the leaves contribute to A_n .
- If vertex 1 is white and vertex 2 is black, see figure 9(b), the colors of the $n - 4$ neighbors of vertex 2 do not influence the number of white vertices having an even number of black neighbors; only the colors of vertex 3 and 4 do. If both of these vertices are black, vertex 1 has three black neighbors, and all 2^{n-4} color assignments of vertex $5, \dots, n$ contribute to A_n . Otherwise, there are two white vertices with an even number of black neighbors, i.e. the remaining $3 \times 2^{n-4}$ color assignments contribute to A_{n-2} .

The first of these four cases has a contribution of $2^{n-2}\delta_{k,n}$ to A_k , while the second case contributes $3 \times 2^{n-4}\delta_{k,n-2} + 2^{n-4}\delta_{k,n}$. Thus, together they yield the term

$$3 \times 2^{n-4}\delta_{k,n-2} + 5 \times 2^{n-4}\delta_{k,n}, \tag{59}$$

in equation (20) from the main text. We continue with the remaining two cases.

- If vertex 1 is black and vertex 2 is white, see figure 9(c), all four color assignments of vertex 3 and 4 (neighbors of vertex 1) contribute to the same SL. There are $\binom{n-4}{b}$ color assignments of the neighbors of vertex 2 with b black neighbors. Since vertex 2 is white, all its $n - 4 - b$ white neighbors have an even number (zero) of black neighbors. If b is odd, vertex 2 also has an even number of black neighbors. In that case, all $4\binom{n-4}{b}$ color assignments contribute to $A_{n-(n-4-b+1)} = A_{b+3}$. If b is even, however, we have $4\binom{n-4}{b}$ color assignments contributing to A_{b+4} because the white vertex 2 has an odd number of black neighbors.
- If both vertex 1 and 2 are white, see figure 9(d), we look at vertex 3 and 4 first. If they are also white, we already have three white vertices (1, 3, and 4) having an even (zero) number of black neighbors. Otherwise, there is exactly one such white vertex among 1, 3, and 4. Again, we distinguish between the $\binom{n-4}{b}$ color assignments of vertex $5, \dots, n$ with exactly b

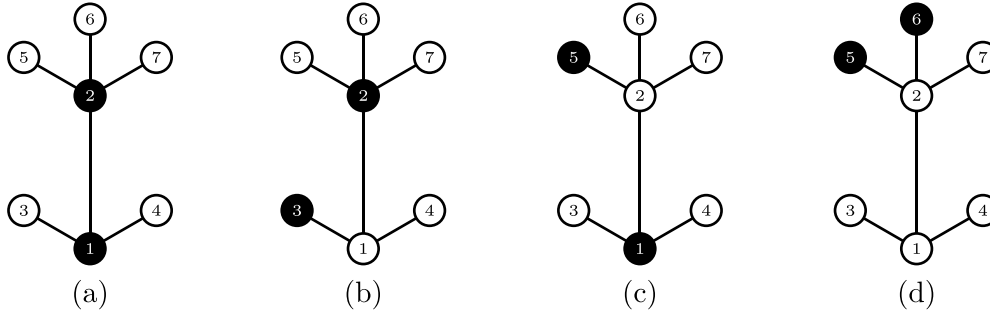


Figure 9. Some black-white color assignments of a Pustoblume graph with $n = 7$ vertices. (a) All color assignments where vertex 1 and 2 are black contribute to A_n . (b) If vertex 1 is white, vertex 2 is black, and vertex 3 is black, there are exactly two white vertices (1 and 4) with an even number of black neighbors, i.e. such a color assignment contributes to A_{n-2} . (c) If vertex 1 is black and vertex 2 is white, every white neighbor of vertex 2 has an even number (zero) of white neighbors. (d) If vertex 1 and 2 are white, the white vertices with an even number of black neighbors are vertex 1, 3, 4, all white neighbors of vertex 2, and possibly vertex 2.

black vertices. If b is odd, the total number of white vertices with an even number of black neighbors is either $(n - 4 - b) + 3$ (if all 1, 3, and 4 are among them) or $(n - 4 - b) + 1$ (if only one vertex among 1, 3, and 4 is white and has an even number of black neighbors). Thus, if b is odd, we have $\binom{n-4}{b}$ color assignments which contribute to A_{b+1} and $3\binom{n-4}{b}$ contributing to A_{b+3} . If b is even, however, the total number of white vertices with an even number of black neighbors is either $(n - 4 - b) + 3 + 1$ or $(n - 4 - b) + 1 + 1$ because now vertex 2 is also one of them. Thus, we have $\binom{n-4}{b}$ color assignments contributing A_b and $3\binom{n-4}{b}$ contributing to A_{b+2} .

We have distinguished between the number $b \in \{0, \dots, n - 4\}$ of the dandelion seed head vertices being black. We find that we only get a contribution to A_k if k is even. From case three, A_k gets a contribution of $4\binom{n-4}{k-4} + 4\binom{n-4}{k-3} = 4\binom{n-3}{k-3}$, where the first and second terms come from the color assignments where $b = k - 4$ and $b = k - 3$, respectively. Similarly, from case four, A_k gets a contribution of $3\binom{n-4}{k-3} + 3\binom{n-4}{k-2} + \binom{n-4}{k-1} + \binom{n-4}{k} = 3\binom{n-3}{k-2} + \binom{n-3}{k}$, if k is even. In total, case three and four have a contribution of

$$\left(\binom{n-3}{k-3} + 3\binom{n-2}{k-2} + \binom{n-3}{k} \right) \delta_{k,\text{even}} \tag{60}$$

to A_k for each k . This finishes the derivation of equation (20) stated in the main text.

Appendix B. Solution of the graph-theoretical problem for the cycle graph

In this appendix, we derive the SLD of the n -qubit RC state, which is stated in equation (21). According to the color assignment problem, A_k is the number of color assignments of the n -vertex cycle graph, see figure 4, such that $n - k$ white vertices have an even number of black neighbors. All possible color assignments are parameterized by the set \mathbb{F}_2^n where $\mathbf{r} \in \mathbb{F}_2^n$ corresponds to the color assignment where vertex $i \in V$ is white if $r_i = 0$ and black if $r_i = 1$. To capture the periodicity of the cycle, we use integers modulo n as the vertex set $V = \mathbb{Z}/n\mathbb{Z}$. Since each vertex of the cycle graph has exactly two neighbors, the condition of having an even



Figure 10. If one distributes $b = b_1 + b_2 + \dots + b_{n-b}$ black vertices into $n - b$ boxes in such a way that no box remains empty, one obtains a color assignment pattern $\mathbf{b} = (b_1, \dots, b_{n-b}) \in \mathcal{B}_{b,n-b}$ of the cycle graph which contributes to $C_{n,b,0}$. By shifting the whole pattern to the left, where periodic boundary conditions are applied, one obtains $1 + b_1$ different color assignments before there is again a white vertex on the leftmost position.

number of black neighbors is equivalent to the condition of both neighbors having the same color. Thus, the number of white vertices fulfilling this condition for a given color assignment $\mathbf{r} \in \mathbb{F}_2^n$ can be expressed as

$$x_1(\mathbf{r}) = |\{i \in V \mid r_i = 0, r_{i-1} = r_{i+1}\}|. \tag{61}$$

By introducing the notation $x_2(\mathbf{r}) = |\{i \in V \mid r_i = 0, r_{i-1} \neq r_{i+1}\}|$ for the number of other white vertices, as well as $x_3(\mathbf{r}) = |\{i \in V \mid r_i = 1\}|$ for the number of black vertices, we obtain the relation $x_1(\mathbf{r}) + x_2(\mathbf{r}) + x_3(\mathbf{r}) = n$. Therefore, the k -body SL A_k is given by the cardinality of the set

$$\mathcal{X}_k = \{\mathbf{r} \in \mathbb{F}_2^n \mid x_1(\mathbf{r}) = n - k\} = \{\mathbf{r} \in \mathbb{F}_2^n \mid x_2(\mathbf{r}) + x_3(\mathbf{r}) = k\}. \tag{62}$$

At each vertex $i \in V$ with $r_{i-1} = 1, r_i = r_{i+1} = 0$ there starts a path of $l_i \geq 2$ white vertices, i.e. $r_{i+2} = \dots = r_{i+l_i} = 0$ but $r_{i+l_i+1} = 1$. The inner vertices contribute to $x_1(\mathbf{r})$ as they have two white neighbors. The two ends of the white path, however, contribute to $x_2(\mathbf{r}) = 2m(\mathbf{r})$, where $m(\mathbf{r})$ is the number of white paths of length $l \geq 2$. By sorting the color assignments $\mathbf{r} \in \mathcal{X}_k$ by $m(\mathbf{r})$, we obtain the disjoint union $\mathcal{X}_k = \bigcup_{m=0}^{\lfloor k/2 \rfloor} \mathcal{X}_k^{(m)}$ into the sets

$$\mathcal{X}_k^{(m)} = \{\mathbf{r} \in \mathbb{F}_2^n \mid x_2(\mathbf{r}) = 2m, x_3(\mathbf{r}) = k - 2m\}. \tag{63}$$

Note that m only runs from 0 to $\lfloor k/2 \rfloor$ because, otherwise, $x_2(\mathbf{r})$ or $x_3(\mathbf{r})$ would be negative. By defining $C_{n,b,m}$ as the number of color assignments of the n -vertex cycle graph with exactly $b \geq 0$ black vertices and exactly $m \geq 0$ white paths of length greater than or equal to 2, we obtain the formal expression

$$A_k = \sum_{m=0}^{\lfloor \frac{k}{2} \rfloor} C_{n,k-2m,m}, \tag{64}$$

which will reduce to equation (21) once we have found explicit formulas for $C_{n,b,m}$.

Let us treat the easy case, $m = 0$, first. If $b = 0$, all vertices must be white and we obtain the trivial SL $A_0 = C_{n,0,0} = 1$, which is fixed by normalization. However, if there is at least one black vertex, $b \geq 1$, the graph-theoretical problem from theorem 1 from the main text can be restated into ‘ $C_{n,b,0}$ is the number of color assignments of the n -vertex cycle graph with exactly b black vertices such that each white vertex has zero white neighbors’ because there are no white paths of length $l \geq 2$. To achieve this condition, b black vertices have to be distributed among the $n - b$ gaps between the white vertices, cf figure 10. The resulting set of possible patterns is given by

$$\mathcal{B}_{b,w} = \left\{ (b_1, \dots, b_w) \in \mathbb{Z}^w \mid \sum_{i=1}^w b_i = b, b_i \geq 1 \right\}, \tag{65}$$

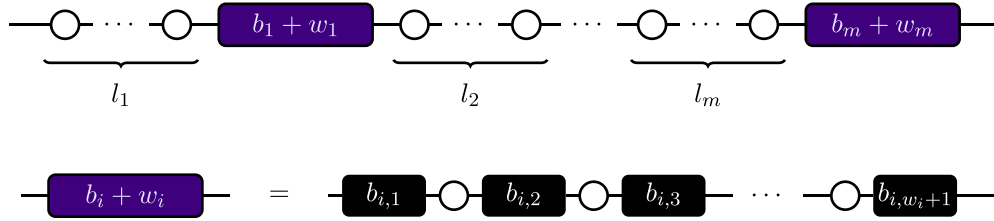


Figure 11. Top: a pattern contributing to $C_{n,b,m}$ consists of m white paths of length $l_i \geq 2$, which are separated by mixed paths of length $b_i + w_i$ as depicted in blue. By shifting the whole pattern to the left, where periodic boundary conditions are applied, one obtains $l_1 + b_1 + w_1$ different color assignments before there is again a white path (of length l_2) starting at the leftmost position. Bottom: in the i th mixed path, each of the w_i white vertices needs two black neighbors. There are $|\mathcal{B}_{b_i, w_i+1}| = \binom{b_i-1}{w_i}$ choices to distribute the $b_i = b_{i,1} + \dots + b_{i, w_i+1}$ black vertices into $w_i + 1$ boxes such that no box remains empty.

where $w = n - b$. We will need the notation introduced in equation (65) for general $w \geq 1$ at a later stage. Via repeated shifts to the left, one obtains $1 + b_1$ different color assignments for each pattern $\mathbf{b} = (b_1, b_2, \dots, b_w) \in \mathcal{B}_{b,w}$. An additional shift would result in a color assignment which is already covered by the pattern $(b_2, \dots, b_w, b_1) \in \mathcal{B}_{b,w}$. Therefore, we find

$$C_{n,b,0} = \sum_{\mathbf{b} \in \mathcal{B}_{b,n-b}} (1 + b_1). \tag{66}$$

By elementary combinatorics, there are $|\mathcal{B}_{b,w}| = \binom{b-1}{w-1}$ possibilities to distribute b unlabeled balls into w labeled boxes such that no box remains empty. After a little algebra, we find the formula (needed later in full generality)

$$\sum_{\mathbf{b} \in \mathcal{B}_{b,w}} (x + b_1 y) = \binom{b-1}{w-1} \left(x + \frac{by}{w} \right), \tag{67}$$

which holds for any choice of $x, y \in \mathbb{R}$ and integers $b \geq 0, m \geq 1$. Setting $w = n - b$ and $x = y = 1$, we obtain $C_{n,b,0} = \frac{n}{b} \binom{b}{n-b}$ which appears as the first term in equation (21).

Now, we solve $C_{n,b,m}$ for $m \geq 1$ white paths of length $l_1, \dots, l_m \geq 2$. For each color assignment, the total number $l = l_1 + \dots + l_m$ of white vertices in the m paths is somewhere in between $2m$ and $n - b$. The number w of isolated white vertices, i.e. white vertices with two black neighbors, is fixed by the relation $w = n - l - b$. As it is depicted in figure 11, these isolated white vertices are part of the mixed paths which separate the white paths of length $l_i \geq 2$ from each other. The mixed path, which separates the white paths of length l_i from the white path of length l_{i+1} , consists of b_i black and w_i white vertices. Since the vertices at the end of the mixed path have to be black and the isolated white vertices are separated by at least one black vertex, there are $|\mathcal{B}_{b_i, w_i+1}| = \binom{b_i-1}{w_i}$ different mixed paths consisting of b_i black and w_i white vertices. In analogy to equation (65), we introduce the sets

$$\mathcal{L}_{l,m} = \left\{ (l_1, \dots, l_m) \in \mathbb{Z}^m \mid \sum_{i=1}^m l_i = l, l_i \geq 2 \right\} \tag{68}$$

$$\text{and } \mathcal{W}_{w,m} = \left\{ (w_1, \dots, w_m) \in \mathbb{Z}^m \mid \sum_{i=1}^m w_i = w, w_i \geq 0 \right\}. \tag{69}$$

The set $\mathcal{L}_{l,m}$ contains all possible lengths for the white paths of a fixed combined length $l \in \{2m, \dots, n - b\}$. The set $\mathcal{W}_{w,m}$ is used to parameterize the possibilities of distributing the remaining $w = n - b - l$ isolated white vertices among the mixed paths. Since there are $\binom{b_i-1}{w_i}$ mixed paths for each choice of b_i and w_i , we obtain $\prod_{i=1}^m \binom{b_i-1}{w_i}$ different mixed-chain color assignments for each choice of $\mathbf{b} = (b_1, \dots, b_m) \in \mathcal{B}_{b,m}$, $\mathbf{w} = (w_1, \dots, w_m) \in \mathcal{W}_{w,m}$. In analogy to our argumentation around the derivation of $C_{n,b,0}$ in equation (66), each pattern $(\mathbf{l}, \mathbf{b}, \mathbf{w}) \in \bigcup_{l=2m}^{n-b} \mathcal{L}_{l,m} \times \mathcal{B}_{b,m} \times \mathcal{W}_{n-l-b,m}$ gives rise to exactly $l_1 + b_1 + w_1$ color assignments if the mixed-chain color assignment is fixed. Combining all of our arguments, we obtain the equation

$$C_{n,b,m} = \sum_{l=2m}^{n-b} \sum_{\mathbf{l} \in \mathcal{L}_{l,m}} \sum_{\mathbf{b} \in \mathcal{B}_{b,m}} \sum_{\mathbf{w} \in \mathcal{W}_{n-l-b,m}} (l_1 + b_1 + w_1) \prod_{i=1}^m \binom{b_i-1}{w_i}. \tag{70}$$

To simplify this expression, we make use of the well-known Vandermonde identity

$$\sum_{\mathbf{w} \in \mathcal{W}_{n-l-b,m}} \prod_{i=1}^m \binom{b_i-1}{w_i} = \binom{b-m}{n-b-l} \tag{71}$$

as well as one of its generalizations [52, equation (8)]

$$\sum_{\mathbf{w} \in \mathcal{W}_{n-l-b,m}} w_1 \prod_{i=1}^m \binom{b_i-1}{w_i} = \binom{b-m}{n-b-l} \frac{(n-b-l)(b_1-1)}{b-m}. \tag{72}$$

By combining equations (70)–(72), we obtain

$$C_{n,b,m} = \sum_{l=2m}^{n-b} \binom{b-m}{n-b-l} \sum_{\mathbf{l} \in \mathcal{L}_{l,m}} \sum_{\mathbf{b} \in \mathcal{B}_{b,m}} \left((l_1 + b_1) + \frac{(n-b-l)(b_1-1)}{b-m} \right) \tag{73}$$

$$= \sum_{l=2m}^{n-b} \binom{b-m}{n-b-l} \sum_{\mathbf{l} \in \mathcal{L}_{l,m}} \sum_{\mathbf{b} \in \mathcal{B}_{b,m}} \left(\left(l_1 - \frac{n-b-l}{b-m} \right) + b_1 \left(1 + \frac{n-b-l}{b-m} \right) \right) \tag{74}$$

$$\stackrel{(67)}{=} \binom{b-1}{m-1} \sum_{l=2m}^{n-b} \binom{b-m}{n-b-l} \sum_{\mathbf{l} \in \mathcal{L}_{l,m}} \left(l_1 - \frac{n-b-l}{b-m} + \frac{b}{m} \left(1 + \frac{n-b-l}{b-m} \right) \right) \tag{75}$$

$$= \binom{b-1}{m-1} \sum_{l=2m}^{n-b} \binom{b-m}{n-b-l} \sum_{\mathbf{l} \in \mathcal{L}_{l,m}} \left(l_1 + \frac{n-l}{m} \right). \tag{76}$$

Similar to equation (67), we can simplify the last term,

$$\sum_{\mathbf{l} \in \mathcal{L}_{l,m}} \left(\frac{n-l}{m} + l_1 \right) = \binom{l-m-1}{m-1} \left(\frac{n-l}{m} + \frac{l}{m} \right) = \binom{l-m-1}{m-1} \frac{n}{m}. \tag{77}$$

Substituting $b = k - 2m$ together with an index shift $l \mapsto l - 2m$ yields

$$C_{n,k-2m,m} = \frac{n}{m} \binom{k-2m-1}{m-1} \sum_{l=0}^{n-k} \binom{k-3m}{n-k-l} \binom{l+m-1}{l}. \tag{78}$$

Inserting this into equation (64), we finally arrive at equation (21) from the main text. Note that it suffices if m runs from 1 to $\lfloor \frac{k-1}{2} \rfloor$ because $\binom{k-2m-1}{m-1} = 0$ if $m \geq \frac{k}{2}$.

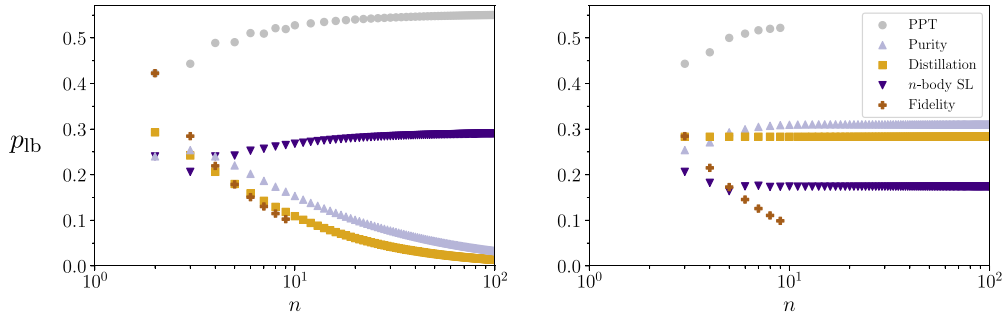


Figure 12. Lower bounds p_{lb} on the local-white-noise entanglement threshold p_{crit} for n -qubit GHZ (left) and RC states (right). The noisy state $\mathcal{E}_{loc}^{(p)}[|\psi\rangle\langle\psi|]$, see equation (45), is entangled iff $p < p_{crit}$, where $|\psi\rangle = |\text{GHZ}(n)\rangle$ and $|\psi\rangle = |\text{RC}(n)\rangle$, respectively.

Appendix C. Lower bounds on entanglement noise thresholds of graph states

In this appendix, we apply corollary 5 from the main text to derive lower bounds on the local-white-noise entanglement threshold for several families of stabilizer states. We start with the qubit case in appendix C.1 and discuss higher-dimensional qudits in appendix C.2.

C.1. Robustness of entanglement in qubit graph states against local white noise

In section 3 of the main text, we show that the normalized SLD of a typical graph state is very close to a binomial distribution. To cover both a special case and the generic case, in figure 12 we plot for n -qubit GHZ (left) and RC states (right) several lower bounds p_{lb} on the local-white-noise entanglement threshold as a function of n . Note that the largest value of p_{lb} in figure 12 corresponds to the strongest entanglement criterion for a given state. We see that the PPT criterion (gray circles) outperforms the other criteria in all cases for which it is available. Whenever n is even, the PPT criterion yields the lower bound,

$$p_{PPT,loc}^{GHZ(n)} = 1 - \frac{1}{\sqrt{2^{2-2/n} + 1}}, \tag{79}$$

on the entanglement noise threshold for n -qubit GHZ states [53]. For GHZ states with odd $n \leq 9$, we compute the PPT bound using a direct approach with exponential runtime. To our knowledge, a result similar to equation (79) is not available for RC states; our direct approach yields $p_{PPT,loc}^{RC(n)}$ for all $n \in \{3, 4, \dots, 9\}$. For $n \geq 10$, the best available lower bound on the noise threshold for $|\text{RC}(n)\rangle$ is based on the purity criterion (lavender upward triangles) and found via corollary 5. Interestingly, the same criterion performs comparatively badly for GHZ states. For them, the second best criterion (after PPT) is given by the n -body SL criterion (blue downward triangles) from equation (55) of the main text. For comparison, we also plot the bound (yellow squares),

$$p_{distill,loc}^{graph} = 1 - 2^{-2/\left(2 + \max_{\{i,j\} \in E} \{\text{deg}(i) + \text{deg}(j)\}\right)}, \tag{80}$$

which is based on an entanglement distillation protocol for graph states $|\Gamma\rangle$ whose set of edges is denoted by E [47]. Finally, we determine the value of p for which the fidelity of the noisy state with the target state, $|\psi\rangle$, is equal to 0.5. If the noise parameter is below this value (brown plusses), the noisy state is GME since the operator $W = \frac{1}{2} - |\psi\rangle\langle\psi|$ is a GME witness [54–57].

As this direct approach also has exponential runtime, we can apply this fidelity criterion only for $n \leq 9$.

In contrast to the unphysical case of global white noise from equation (54), all entanglement criteria considered in figure 12 yield physically meaningful local-noise thresholds that are smaller than 1, e.g. $\lim_{n \rightarrow \infty} p_{\text{PPT,loc}}^{\text{GHZ}(n)} = 1 - 1/\sqrt{5} \approx 0.553$ and $\lim_{n \rightarrow \infty} p_{n\text{SL,loc}}^{\text{GHZ}} = 1 - 1/\sqrt{2} \approx 0.293$. The latter is larger than $\lim_{n \rightarrow \infty} p_{n\text{SL,loc}}^{\text{RC}(n)} \approx 0.174$ because $A_n^{\text{GHZ}(n)} = 2^{n-1} + \delta_{n,\text{even}}$ exceeds

$$A_n^{\text{RC}(n)} = 1 + \sum_{k=1}^{\lfloor n/3 \rfloor} \binom{n-2k-1}{k-1} \frac{n}{k}. \quad (81)$$

Note that equation (81) is a simplified special case of equation (21) of the main text. Next, we point out that for qubits, theorem 4 simplifies to:

$$\sum_{k=0}^{\lfloor n/2 \rfloor} (n-2k)A_k[\rho] < \sum_{k=\lceil n/2 \rceil}^n (2k-n)A_k[\rho] \implies \rho \text{ is entangled.} \quad (82)$$

In other words, ρ is entangled if the (slightly rescaled) k -body SLs with $k > n/2$ outperform those with $k < n/2$, which is intuitive because A_k quantifies k -body correlations and entanglement is a strong form of correlation. For the GHZ state, the most important contribution to the k -body SLs with $k > n/2$ is A_n . We attribute the observation that $p_{\text{pur,loc}}^{\text{GHZ}(n)}$ from corollary 5 converges to zero in figure 12 to the fact that A_n declines extremely fast, recall equation (53). For RC states, on the other hand, the normalized SLD is close to a binomial distribution centered at $3n/4$. Since the k -body SL decline around $k = 3n/4$ is not as severe as for $k \approx n$, this causes the corresponding lower bound from corollary 5 to numerically converge to $\lim_{n \rightarrow \infty} p_{\text{pur,loc}}^{\text{RC}(n)} \approx 0.310$, which to our knowledge is the best available lower bound on the noise threshold for RC states⁷. It is closely followed by $p_{\text{distill,loc}}^{\text{RC}(n)} \approx 0.283$, which is constant because the degrees of the vertices in a cycle graph C_n are independent of n [47]. For the star graph $K_{1,n-1}$, on the other hand, the degree of the central vertex is unbounded, which causes $p_{\text{distill,loc}}^{\text{GHZ}(n)}$ to converge to zero [47].

Finally, consider the bound that is based on the fidelity criterion. Since this criterion can be used to certify GME, it is often employed in experiments [58–61]. As we can see in figure 12, the level of noise that is required to successfully apply the fidelity criterion in such an experiment decreases in n . This is bad news for benchmarkers of quantum processors in which errors are accurately modeled by local white noise because the qubits have to become less noisy (in the next generation of the quantum processor with an increased number of qubits) to verify GME via fidelity measurements. This is very demanding for near-term quantum hardware. The n -body SL for the verification of (possibly biseparable) entanglement, on the other hand, has critical noise thresholds well above ten percent, independent of the number of qubits.

C.2. Robustness of entanglement in qudit graph states against local white noise

For the sake of completeness, let us also apply the results developed in this paper to the general case of qudits in dimension $d \geq 2$. The only bound on the local-white-noise threshold of an

⁷ The minor differences between the two distributions in figure 5 that are discussed in section 2.3 would lead to an overestimation of the SL-based noise thresholds: For a hypothetical state with $\mathbf{a}^{\text{hypo}} = \mathbf{b}(p = 3/4)$, we would find $\lim_{n \rightarrow \infty} p_{\text{pur,loc}}^{\text{hypo}} \approx 0.423$ and $\lim_{n \rightarrow \infty} p_{n\text{SL,loc}}^{\text{hypo}} \approx 0.184$. For this reason, the approximation $\mathbf{a}^{\text{RC}(n)} \approx \mathbf{b}(3/4)$ and its analogues for other generic graph states should only be used with care.

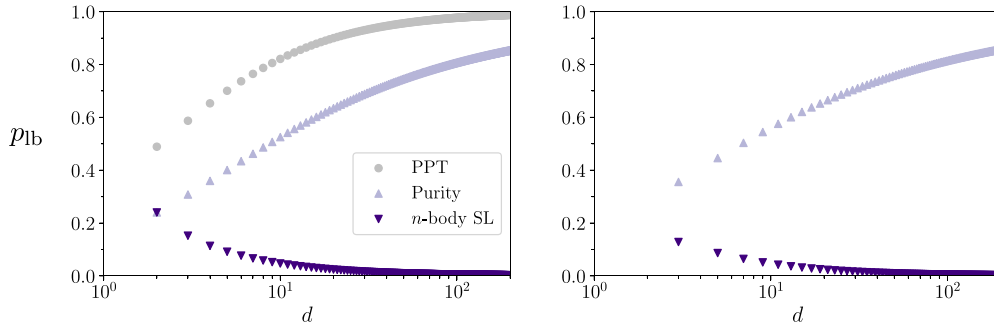


Figure 13. Lower bounds p_{lb} on the local-white-noise entanglement threshold p_{crit} for four-qudit GHZ (left) and AME states (right) as a function of the qudit dimension. The noisy state $\mathcal{E}_{loc}^{(p)}[|\psi\rangle\langle\psi|]$ is entangled iff $p < p_{crit}$, where $|\psi\rangle = |\text{GHZ}_d(4)\rangle$ or $|\psi\rangle = |\text{RC}_d(4)\rangle$.

n -qudit state that we were able to find in the literature applies to the n -qudit GHZ state, as defined in equation (34). It is given by

$$p_{PPT,loc}^{\text{GHZ}_d(n)} = \frac{2d}{\sqrt[n]{4} + \sqrt[n]{2}\sqrt{4 + \sqrt[n]{2d}} + 2d} \tag{83}$$

and holds for arbitrary d and even n [62]. Note that equation (79) is a special case of equation (83). As we show in the left panel of figure 13 for the example of $n = 4$ qubits, the PPT bound (gray circles) converges to 1 in the limit of $d \rightarrow \infty$. The same trend is recovered by the bound based on the purity criterion (lavender upward triangles), which is obtained by applying corollary 5 for the SLD of $|\text{GHZ}_d(n)\rangle$ from equation (35). We also display the bound based on the n -body SL criterion from equation (55) of the main text (blue downward triangles), which converges to zero; this is consistent with the previous observation of the discrepancy between entanglement and A_n in the qudit case [11]. As in the qubit case, the PPT criterion always leads to the best lower bound on the entanglement noise threshold.

For states where the PPT criterion is not solved, our SL-based approaches still work provided the SLD of the investigated state is known. Consider, for example, the four-qudit absolutely maximally entangled (AME) state $|\text{RC}_d(4)\rangle$, which is defined for odd d in equation (101). We present its SLD in equation (102) of appendix F and plot the corresponding lower bounds on the local-white-noise threshold in the right panel of figure 13. As in the case of four-qudit GHZ states, we find that the bound based on the n -body SL criterion decreases, whereas the purity bound increases in d . This demonstrates the usefulness of corollary 5 in the case of higher-dimensional qudits.

Appendix D. SLDs of W states as an example of the non-stabilizer case

In the main text, we almost exclusively discuss SLDs of stabilizer states. Since such states constitute only a finite subset of the 2^n -dimensional state space of an n -qubit system, not all of our results apply in the general case. In this appendix, we highlight some important differences using the example of W states [63]. The n -qubit W state is defined as

$$|W(n)\rangle = \frac{1}{\sqrt{n}} \sum_{i=1}^n |\mathbf{e}_i\rangle, \tag{84}$$

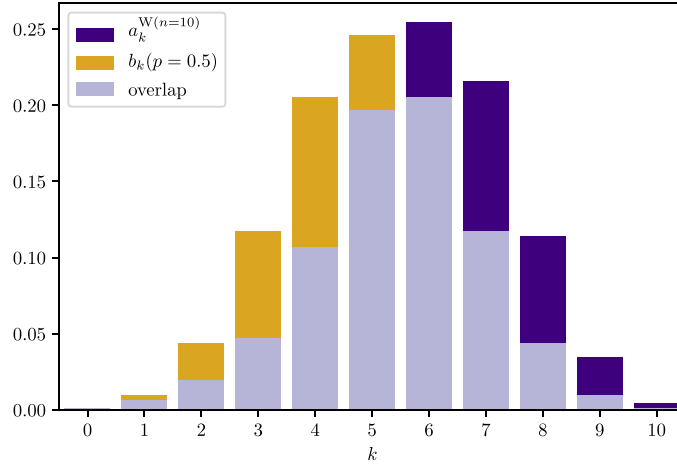


Figure 14. Comparison of the normalized SLD $a_k^{W(n)} = 2^{-n}A_k^{W(n)}$ of the W state from equation (85) to the symmetric binomial distribution $b_k(p = 0.5) = \binom{n}{k}2^{-n}$ for $n = 10$. The latter coincides with the normalized SLD of a fully separable state, i.e. $\mathbf{b}(p = 0.5) = \mathbf{a}^{\text{sep}(n)}$.

where $\mathbf{e}_1 = (1, 0, \dots, 0), \dots, \mathbf{e}_n = (0, \dots, 0, 1)$ is the standard basis of \mathbb{F}_2^n . For $n \geq 3$, the W state is not a (Pauli) stabilizer state. While the definition of the k -body SL in equation (3) is applicable to any n -qubit state, only in the case of a pure stabilizer state is A_k guaranteed to be an integer. The k -body SL of $|W(n)\rangle$, on the other hand, is given by

$$A_k^{W(n)} = \binom{n}{k} \left(1 + \frac{4k}{n^2} (2k - n - 1) \right), \tag{85}$$

see equation (18) of [6] for the more general case of Dicke states. For $n \geq 3$, it can happen that $A_k^{W(n)}$ is not an integer, e.g. $\mathbf{A}^{W(5)} = (1, 1.8, 3.6, 10, 11.4, 4.2)$. However, there are also non-stabilizer states for which the SLD takes integer values, e.g. $\mathbf{A}^{W(4)} = (1, 1, 3, 7, 4)$. Interestingly, $|W(4)\rangle$ has exactly the same SLD as the only stabilizer state (up to LU-equivalence) for which $A_1 = I = 1$, namely $|+\rangle \otimes |\text{GHZ}(3)\rangle$.

For pure stabilizer states, we establish in equation (9) that A_1^{stab} is the number of qubits that are disentangled from all other qubits. In particular, $A_1^{\text{stab}} \geq 1$ implies that the stabilizer state is separable. The W state, however, has a 1-body SL of $A_1^{W(n)} = (n - 2)^2/n$. In particular, we have $A_1^{W(n)} \geq 1$ for all $n \geq 4$, despite $|W(n)\rangle$ being GME.

Note that the mean $\langle k \rangle_{\mathbf{a}^{W(n)}} = (n^2 + 2n - 4)/2n$ can still be inferred from $A_1^{W(n)}$ via equation (16) from the main text because MacWilliams identities hold for arbitrary pure states. While GME stabilizer states obey $\langle k \rangle_{\mathbf{a}^{\text{stab}}}/n = 3/4$ for all n , we find $\langle k \rangle_{\mathbf{a}^{W(n)}}/n \rightarrow 1/2$ for $n \rightarrow \infty$. In figure 14, we plot the normalized SLD $\mathbf{a}^{W(n)}$ (blue) and the symmetrical binomial distribution \mathbf{b} (yellow) with $b_k = \frac{1}{2^n} \binom{n}{k}$ for the example of $n = 10$ qubits. Although the mean $\langle k \rangle_{\mathbf{a}^{W(10)}} = 5.9$ of $\mathbf{a}^{W(n)}$ is still notably larger than $\langle k \rangle_{\mathbf{b}} = 5$, the two distributions exhibit a considerable overlap (lavender). In the main text, section 3.1, we plot the TVD between $\mathbf{a}^{W(n)}$ and \mathbf{b} as a function of n (lavender curve in figure 7). There, we observe that the curve decreases with n . This is unsurprising because the difference of the normalized Bloch vectors of $|W(n)\rangle$ and $|0\rangle^{\otimes n}$ converges to zero in the limit of $n \rightarrow \infty$; see supplemental material of [64] for the Bloch vector components of $|W(n)\rangle$.

Let us rigorously show that $\text{TVD}(\mathbf{a}^{W(n)}, \mathbf{b})$ converges to zero. For simplicity, we write $\mathbf{a} = \mathbf{a}^{W(n)}$. From equation (85), we can see that $a_k \geq b_k$ is equivalent to $2k \geq n + 1$. Thus, we can split the sum in equation (22) to avoid absolute values, which yields

$$\text{TVD}(\mathbf{a}, \mathbf{b}) = \frac{1}{2} \left(\sum_{k=0}^{\lfloor \frac{n}{2} \rfloor - 1} (b_k - a_k) + \sum_{k=\lfloor \frac{n}{2} \rfloor + 1}^n (a_k - b_k) \right) + \frac{b_{n/2} - a_{n/2}}{2} \delta_{n,\text{even}}. \quad (86)$$

After substituting $k \mapsto n - k$ in the second sum and exploiting the fact that all terms of the form $b_k - b_{n-k}$ vanish, we can rewrite equation (86) as

$$\text{TVD}(\mathbf{a}, \mathbf{b}) = \frac{1}{2} \sum_{k=0}^{\lfloor \frac{n}{2} \rfloor - 1} (a_{n-k} - a_k) + \frac{1}{2^n n} \binom{n}{\frac{n}{2}} \delta_{n,\text{even}}, \quad (87)$$

where we also used $a_{n/2} - b_{n/2} = \frac{2}{2^n n} \binom{n}{n/2}$ for the case of n even. Next, we find

$$a_{n-k} - a_k = \frac{n-1}{2^{n-2} n^2} \binom{n}{k} (n-2k) \quad (88)$$

by exploiting equation (85). In combination with $\sum_{k=0}^{\lfloor \frac{n}{2} \rfloor - 1} (n-2k) = \lfloor \frac{n}{2} \rfloor \binom{n}{\lfloor \frac{n}{2} \rfloor}$, this yields

$$\text{TVD}(\mathbf{a}, \mathbf{b}) = \frac{n-1}{2^{n-1} n^2} \lfloor \frac{n}{2} \rfloor \binom{n}{\lfloor \frac{n}{2} \rfloor} + \frac{1}{2^n n} \binom{n}{\frac{n}{2}} \delta_{n,\text{even}}. \quad (89)$$

In the case of even n , Stirling's formula allows us to rewrite equation (89) as

$$\text{TVD}(\mathbf{a}, \mathbf{b}) = \frac{1}{2^n} \binom{n}{\frac{n}{2}} \propto \frac{1}{\sqrt{n}} \xrightarrow{n \rightarrow \infty} 0. \quad (90)$$

Similarly, equation (89) simplifies to $\text{TVD}(\mathbf{a}, \mathbf{b}) = \frac{n^2-1}{2^n n^2} \binom{n}{(n-1)/2} \propto 1/\sqrt{n}$ if n is odd. This establishes that $\text{TVD}(\mathbf{a}^{W(n)}, \mathbf{b}(p=0.5))$ converges to zero as $1/\sqrt{n}$. Recall from figure 7, that we have strong numerical evidence that $\text{TVD}(\mathbf{a}^{\text{RC}(n)}, \mathbf{b}(p=0.75))$ features the same behavior. Conducting a more detailed study of such convergence effects could be a worthwhile endeavor as it may further strengthen our understanding of SLDs.

Appendix E. Expected SLD for random graph states

Here, we derive equation (25) from the main text. The expected k -body SL of an Erdős–Rényi graph state with n vertices and edge-probability q is given by

$$\langle A_k \rangle_q = \sum_{\Gamma \in \mathcal{G}} \text{Pr}[\Gamma_n^{(q)} = \Gamma] A_k[|\Gamma\rangle\langle\Gamma|], \quad (91)$$

where $\mathcal{G} \subset \mathbb{F}_2^{n \times n}$ denotes the set of all adjacency matrices. Inserting equation (11) into equation (91) allows us to write

$$\langle A_k \rangle_q = \sum_{b=0}^k \sum_{\mathbf{r} \in \mathcal{B}_b} \sum_{\Gamma \in \mathcal{G}} \text{Pr}[\Gamma_n^{(q)} = \Gamma] \delta_{\text{swt}(\mathbf{r}, \Gamma), k} \quad (92)$$

as a sum over all color assignments $\mathbf{r} \in \mathbb{F}_2^n$ with an increasing number $b \leq k$ of black vertices. As $\text{Pr}[\Gamma_n^{(q)} = \Gamma]$ is invariant under renumeration of the vertices of Γ , we can replace \mathbf{r} by the color assignment $\mathbf{r}_b = (1, \dots, 1, 0, \dots, 0)$ for which the first b vertices are black, while the

other $n - b$ vertices are white. Since there are $|\mathcal{B}_b| = \binom{n}{b}$ color assignments with exactly b black vertices, we can restate equation (92) as

$$\langle A_k \rangle_q = \sum_{b=0}^k \binom{n}{b} p(n, q, b, k), \quad (93)$$

where $p(n, q, b, k) = \sum_{\Gamma \in \mathcal{G}} \Pr[\Gamma_n^{(q)} = \Gamma] \delta_{\text{swt}(\mathbf{r}_b, \Gamma \mathbf{r}_b), k}$ denotes the probability that a graph with b black vertices has exactly $n - k$ white vertices with an even number of black neighbors; recall theorem 1. For any given white vertex, the probability of having an even number of black neighbors is given by

$$p_{\text{even}}(q, b) = \sum_{\substack{a=0 \\ a \text{ even}}}^b \binom{b}{a} q^a (1 - q)^{b-a} = \frac{1 + (1 - 2q)^b}{2} \quad (94)$$

because every edge (between the given white vertex and any of the black vertices) is present with probability q . Since this probability is independently the same for each of the $n - b$ white vertices, the probability that exactly $n - k$ of them have the desired property follows as

$$p(n, q, b, k) = \binom{n-b}{n-k} p_{\text{even}}(n, q, b)^{n-k} (1 - p_{\text{even}}(n, q, b))^{k-b}. \quad (95)$$

Inserting equations (94) and (95) into equation (93) yields equation (25) from the main text.

Appendix F. Graph-theoretical treatment of SLDs of qudit graph states

In this appendix, we discuss what information about the SLD of a qudit graph state $|\Gamma\rangle$, as defined in equation (36) of the main text, one can directly infer from the graph Γ . Since the stabilizer group

$$\mathcal{S} = \left\{ X_d^{\mathbf{r}} Z_d^{\Gamma \mathbf{r}} \omega_d^{\sum_{i < j} r_i \gamma_{i,j} r_j} \mid \mathbf{r} \in (\mathbb{Z}/d\mathbb{Z})^n \right\} \quad (96)$$

of $|\Gamma\rangle$ is parameterized by the color assignments $\mathbf{r} \in (\mathbb{Z}/d\mathbb{Z})^n$ of Γ (with d colors), we can state

$$A_k = |\{\mathbf{r} \in (\mathbb{Z}/d\mathbb{Z})^n \mid \text{swt}_d(\mathbf{r}, \Gamma \mathbf{r}) = k\}|, \quad (97)$$

which generalizes equation (8) from the main text. However, only if d and n are small enough, it is feasible to iterate through all d^n color assignments to compute the SLD $\mathbf{A} = (A_0, \dots, A_n)$ via equation (97). Since only color assignments with $b \leq k$ non-white ($r_i \neq 0$) vertices i can contribute to A_k , we find for n -qudit graph states the bound

$$A_k \leq \sum_{b=1}^k \binom{n}{k} (d - 1)^b, \quad (98)$$

which generalizes equation (12) from the main text, where $k \geq 1$. Since SLDs are convex, equation (98) also holds for mixtures of graph states. If d is prime, every stabilizer state is LU-equivalent to a graph state [33]. This implies the validity of the bound in equation (98) for all mixtures of arbitrary n -qudit stabilizer states.

For qudits in prime dimension d , one can relate A_1 and A_2 to graph-theoretical notions: the 1-body SL is equal to the number of color assignments where exactly one vertex $j \in \{1, \dots, n\}$ obeys $r_j \neq 0$ and all other vertices $i \neq j$ fulfill $\gamma_{i,j} r_j = 0$. Here, $\mathbb{Z}/d\mathbb{Z} = \mathbb{F}_d$ is a field. Thus, $\gamma_{i,j} r_j = 0$ is equivalent to $\gamma_{i,j} = 0$, i.e. i is an isolated vertex. Since there are $d - 1$ choices for

$r_j \neq 0$, we find $A_1 = (d - 1)I$, as mentioned in equation (41) of the main text. For the 2-body SL, two types of color assignments $\mathbf{r} \in \mathbb{F}_d^n$ can contribute: either one or two vertices are not colored white. If there is exactly one vertex $j \in \{1, \dots, n\}$ with $r_j \neq 0$, there has to be exactly one other vertex $i \neq j$ with $\gamma_{i,j}r_j \neq 0$. Since \mathbb{F}_d is a field, the latter is equivalent to $\gamma_{i,j} \neq 0$. Therefore, such a color assignment contributes iff j has exactly one neighbor, i.e. j is a leaf. This yields exactly $(d - 1)L$ color assignments of the first type that contribute to A_2 , where L is the number of leaves. For the second type of color assignments $\mathbf{r} \in \mathbb{F}_d^n$, which have exactly two vertices $j \neq j'$ with $r_j, r_{j'} \neq 0$, the property in equation (40) simplifies to: a color assignment \mathbf{r} contributes to A_2 iff

$$\gamma_{i,j}r_j = -\gamma_{i,j'}r_{j'} \tag{99}$$

for all $i \in \{1, \dots, n\} \setminus \{j, j'\}$. If $\gamma_{i,j} \neq 0$, for a given vertex i , then equation (99) can only be fulfilled if $\gamma_{i,j'} \neq 0$ because \mathbb{F}_d is a field. This implies that only *twin pairs*, i.e. pairs of vertices (j, j') with the same neighborhood, have the potential to contribute to A_2 ; note that $\gamma_{i,j} \neq \gamma_{i,j'}$ is allowed here. We denote the number of twin pairs with exactly $m \in \{0, \dots, n - 2\}$ common neighbors as

$$T_m = \left| \left\{ \{j, j'\} \subset \{1, \dots, n\} \mid j \neq j', m = \left| \{i \in \{1, \dots, n\} \setminus \{j, j'\} \mid \gamma_{i,j}, \gamma_{i,j'} \neq 0\} \right| \right\} \right|. \tag{100}$$

Every twin pair with exactly $m = 0$ common neighbors, of which there are $T_0 = \binom{n}{2}$, contributes with $(d - 1)^2$ color assignments because equation (99) is trivially fulfilled for every choice of $(r_j, r_{j'}) \in (\mathbb{Z}/d\mathbb{Z})^2$. Every twin pair with exactly $m = 1$ common neighbors contributes with exactly $d - 1$ color assignments because one can freely pick $r_j \neq 0$ but $r_{j'} = -\gamma_{i,j}r_j/\gamma_{i,j'}$ is fully determined by the other parameters. All of these considerations lead to the lower bound on A_2 in equation (42) of the main text, which is tight if $T_2 = \dots = T_{n-2} = 0$, e.g. if Γ does not feature any cycles of length 4. In general, however, $T_m \geq 0$ for $m \geq 2$. Then, $r_{j'} = -\gamma_{i,j}r_j/\gamma_{i,j'}$ is again fully determined by r_j , where i is one of the shared neighbors of j and j' . However, the color assignment \mathbf{r} only contributes to A_2 if equation (99) is fulfilled for all common neighbors i of j and j' ; this may or may not happen. If it happens, there are again $d - 1$ color assignments per valid twin pair. This establishes the upper bound on A_2 in equation (42) of the main text.

Consider, for example, the qudit generalization $|\text{RC}_d(n = 4)\rangle$ of the four-qubit RC state for which the adjacency matrix is given by

$$\text{RC}_d(4) = \begin{bmatrix} 0 & +1 & 0 & -1 \\ +1 & 0 & +1 & 0 \\ 0 & +1 & 0 & +1 \\ -1 & 0 & +1 & 0 \end{bmatrix}. \tag{101}$$

This graph has $I = 0$ isolated vertices, $L = 0$ leaves, $T_2 = 2$ twin pairs with two common neighbors, and $T_m = 0$ twin pairs with $m \neq 2$ common neighbors. For every choice of $d \geq 2$ (prime or not), all edges have invertible weights. Hence, the only possibility for a color assignment $\mathbf{r} = (r_1, r_2, r_3, r_4) \in \mathbb{Z}/d\mathbb{Z}$ to contribute to $A_2^{\text{RC}_d(4)}$ is if one pair of twin pairs is white, while the other is not; without loss of generality, $r_1, r_3 \neq 0$ and $r_2 = r_4 = 0$. Additionally, the induced Z-operators on the qudits 2 and 4 must cancel, i.e. $r_1 + r_3 = 0$ and $r_1 - r_3 = 0$, which can only be solved if d is even. Therefore, $A_2^{\text{RC}_d(4)} = 0$ for all odd d . Since $I = 0$ implies that $A_1^{\text{RC}_d(4)} = 0$ also, we recover the well-known fact that all 2-body marginals of $|\text{RC}_d(4)\rangle$ are maximally mixed, i.e. $|\text{RC}_d(4)\rangle$ is AME [65]. In proposition 11 of [27], we computed the SLD of this AME state for arbitrary odd d ,

$$\mathbf{A}^{\text{RC}_d(4)} = (1, 0, 0, 4(d^2 - 1), d^4 - 4(d^2 - 1) - 1). \tag{102}$$

From now on, consider the case of a general n -qudit graph state for which the dimension d is a composite number. Then, $\mathbb{Z}/d\mathbb{Z}$ contains zero divisors, which causes the SLD problem to change from being mainly graph-theoretical to mainly algebraic in nature. For simplicity, we limit our discussion to the case $k = 1$, where only color assignments with $n - 1$ white vertices contribute to A_1 . For the vertex j which is not white, there are $d - 1$ choices for $r_j \neq 0$ and, if j is isolated, all of them contribute. Thus, we obtain a lower bound for arbitrary d ,

$$A_1 \geq (d - 1)I, \tag{103}$$

which is a generalization of equation (41). For composite d , the bound in equation (103) is not necessarily tight, e.g. if $d = 6$, $n = 2$, and $\gamma_{1,2} = 2$, then there are $I = 0$ isolated vertices but the color assignment $\mathbf{r} = (3, 0)$ still contributes to $A_1 = 2$ because $r_1\gamma_{1,2} = 0$ modulo 6, and similarly for $\mathbf{r} = (0, 3)$. For an arbitrary n -qudit graph state, we find for general d ,

$$A_1 = \sum_{i=1}^n |\{r \in \mathbb{Z}/d\mathbb{Z} \mid r \neq 0 \text{ and } (r\gamma_{1,i}, \dots, r\gamma_{n,i}) = (0, \dots, 0)\}|, \tag{104}$$

or, using notions from commutative algebra [66],

$$A_1 = \sum_{i=1}^n |\text{Ann}_{\mathbb{Z}/d\mathbb{Z}}(\Gamma \mathbf{e}_i) \setminus \{0\}|, \tag{105}$$

where $\text{Ann}_R(x)$ denotes the annihilator of an element $x \in M$ in a module M over a ring R , and \mathbf{e}_i is the i th standard basis element of $(\mathbb{Z}/d\mathbb{Z})^n$, i.e. $\Gamma \mathbf{e}_i \in (\mathbb{Z}/d\mathbb{Z})^n$ is the i th column of the adjacency matrix Γ . If $x \neq 0$, then $\text{Ann}_R(x)$ cannot contain any invertible elements; we find $|\text{Ann}_{\mathbb{Z}/d\mathbb{Z}}(\Gamma \mathbf{e}_i)| \leq d - \varphi(d)$, where φ is Euler's totient function, i.e. $\varphi(d)$ is the number of invertible elements in $\mathbb{Z}/d\mathbb{Z}$. This yields an upper bound for general d ,

$$A_1 \leq I(d - 1) + (n - I)(d - 1 - \varphi(d)). \tag{106}$$

Note that the second term in equation (106) vanishes if d is a prime. In this case, the bounds in equations (103) and (106) combine to the result stated in equation (41) of the main text.

Appendix G. Proof of theorem 4

In this appendix, we derive a new family of SLD-based entanglement criteria. The purity criterion [5] states that every fully separable n -qudit state ρ obeys

$$\text{Tr}[\rho^2] \leq \text{Tr}[\text{Tr}_J[\rho]^2], \tag{107}$$

where $J \subset \{1, \dots, n\}$ is a subset of parties and $\text{Tr}_J[\rho]$ is the reduced density matrix of the complementary system $J^C = \{1, \dots, n\} \setminus J$. Using the expansion in equation (27), the marginal state can be written as

$$\text{Tr}_J[\rho] = \sum_{\mathbf{l} \in (\mathbb{Z}/d\mathbb{Z})^m} \frac{1}{d^n} \sum_{\mathbf{r}, \mathbf{s} \in (\mathbb{Z}/d\mathbb{Z})^n} \rho_{\mathbf{r}, \mathbf{s}} \langle \mathbf{l} | X_d^{\mathbf{r}} Z_d^{\mathbf{s}} | \mathbf{l} \rangle_J \tag{108}$$

$$= \frac{1}{d^n} \sum_{\mathbf{r}, \mathbf{s} \in (\mathbb{Z}/d\mathbb{Z})^n} \rho_{\mathbf{r}, \mathbf{s}} X_d^{\mathbf{r} | J} Z_d^{\mathbf{s} | J} \underbrace{\sum_{\mathbf{l} \in (\mathbb{Z}/d\mathbb{Z})^m} \omega_d^{\mathbf{s} | J \cdot \mathbf{l}} \langle \mathbf{l} | \mathbf{r} | J + \mathbf{l} \rangle}_{= \delta_{\mathbf{r} | J, 0} \delta_{\mathbf{s} | J, 0} d^m} \tag{109}$$

$$= \frac{1}{d^{n-m}} \sum_{\substack{\mathbf{r}, \mathbf{s} \in (\mathbb{Z}/d\mathbb{Z})^n \\ \forall j \in J: r_j = s_j = 0}} \rho_{\mathbf{r}, \mathbf{s}} X_d^{\mathbf{r}|_J} Z_d^{\mathbf{s}|_J}, \tag{110}$$

where $\mathbf{r}|_J = (r_{j_1}, \dots, r_{j_m})$ denotes the restriction of \mathbf{r} to $J = \{j_1, \dots, j_m\}$ and likewise for $\mathbf{s}|_J$. Consequently, the right-hand side of equation (107) takes the form

$$\text{Tr} [\text{Tr}_J[\rho]^2] = \frac{1}{d^{n-m}} \sum_{\substack{\mathbf{r}, \mathbf{s} \in (\mathbb{Z}/d\mathbb{Z})^n \\ \forall j \in J: r_j = s_j = 0}} |\rho_{\mathbf{r}, \mathbf{s}}|^2. \tag{111}$$

In the next step of our derivation, we sum up equation (107) for all choices of $J \subset \{1, \dots, n\}$ with $|J| = m$. The right-hand side becomes

$$\sum_{\substack{J \subset \{1, \dots, n\} \\ |J|=m}} \text{Tr} [\text{Tr}_J[\rho]^2] = \frac{1}{d^{n-m}} \sum_{\substack{J \subset \{1, \dots, n\} \\ |J|=m}} \sum_{\substack{\mathbf{r}, \mathbf{s} \in (\mathbb{Z}/d\mathbb{Z})^n \\ \forall j \in J: r_j = s_j = 0}} |\rho_{\mathbf{r}, \mathbf{s}}|^2 \tag{112}$$

$$= \frac{1}{d^{n-m}} \sum_{k=0}^{n-m} \sum_{\substack{J \subset \{1, \dots, n\} \\ |J|=m}} \sum_{\substack{\mathbf{r}, \mathbf{s} \in (\mathbb{Z}/d\mathbb{Z})^n \\ \forall j \in J: r_j = s_j = 0 \\ \text{swt}_d(\mathbf{r}, \mathbf{s})=k}} |\rho_{\mathbf{r}, \mathbf{s}}|^2. \tag{113}$$

For each choice of k and J , there are

$$|\{\mathbf{r}, \mathbf{s} \in (\mathbb{Z}/d\mathbb{Z})^n \mid \forall j \in J: r_j = s_j = 0, \text{swt}_d(\mathbf{r}, \mathbf{s}) = k\}| = \binom{n-m}{k} (d^2 - 1)^k \tag{114}$$

terms in the inner sum of equation (113) as there are $\binom{n-m}{k}$ choices for k indices $i \in \{1, \dots, n\} \setminus J$ with $(r_i, s_i) \neq (0, 0)$ and, for each such choice, there are $(d^2 - 1)^k$ choices for the values of the nonzero entries of (\mathbf{r}, \mathbf{s}) . Hence, there are $\binom{n}{m} \binom{n-m}{k} (d^2 - 1)^k = \binom{n-k}{m} \binom{n}{k} (d^2 - 1)^k$ terms in the inner two sums of equation (113) for each $k \in \{0, \dots, n-m\}$. In contrast, there are only $\binom{n}{k} (d^2 - 1)^k$ terms in the sum of equation (29). Due to our symmetrization, we thus find

$$\sum_{\substack{J \subset \{1, \dots, n\} \\ |J|=m}} \text{Tr} [\text{Tr}_J[\rho]^2] = \frac{1}{d^{n-m}} \sum_{k=0}^n \binom{n-k}{m} A_k, \tag{115}$$

where, again, we have used the convention $\binom{n-k}{m} = 0$ for all $m > n - k$. A similar calculation leads to

$$\sum_{\substack{J \subset \{1, \dots, n\} \\ |J|=m}} \text{Tr}[\rho^2] = \binom{n}{m} \frac{1}{d^n} \sum_{k=0}^n A_k. \tag{116}$$

Since, for a fully separable state, the expression in equation (115) is always larger than the one in equation (116), it follows that every state ρ with

$$\sum_{k=0}^n \left(\binom{n}{m} - d^m \binom{n-k}{m} \right) A_k[\rho] > 0 \tag{117}$$

is entangled. As we explain next, we have numerical evidence that the criterion in equation (117) is strongest if $m = 1$. In this case, equation (117) simplifies to theorem 4.

Our numerical evidence is as follows. We draw n -qubit states at random from the Haar distribution. Then, we compute its SLD via equation (3). For every $m \in \{1, \dots, n-1\}$, we compute the noise threshold below which Ineq. (117) is satisfied using a straightforward generalization of corollary 5. We run this test for 1000 random per qubit numbers for all $n \in \{3, 4, 5, 6, 7, 8\}$. In every single case, we find that the noise threshold is a strictly decreasing function of m .

ORCID iDs

Daniel Miller  <https://orcid.org/0000-0003-2100-5612>

Daniel Loss  <https://orcid.org/0000-0001-5176-3073>

Ivano Tavernelli  <https://orcid.org/0000-0001-5690-1981>

Hermann Kampermann  <https://orcid.org/0000-0002-0659-6699>

Nikolai Wyderka  <https://orcid.org/0000-0003-3002-9878>

References

- [1] Shor P and Laflamme R 1997 Quantum analog of the MacWilliams identities for classical coding theory *Phys. Rev. Lett.* **78** 1600
- [2] Gottesman D 1997 Stabilizer codes and quantum error correction *Caltech PhD Thesis* (arXiv:quant-ph/9705052)
- [3] Scott A J 2004 Multipartite entanglement, quantum-error-correcting codes and entangling power of quantum evolutions *Phys. Rev. A* **69** 052330
- [4] Raïssi Z, Burchardt A and Barnes E 2022 General stabilizer approach for constructing highly entangled graph states *Phys. Rev. A* **106** 062424
- [5] Horodecki R, Horodecki P, Horodecki M and Horodecki K 2009 Quantum entanglement *Rev. Mod. Phys.* **81** 865
- [6] Aschauer H, Calsamiglia J, Hein M and Briegel H J 2004 Local invariants for multi-partite entangled states allowing for a simple entanglement criterion *Quantum Inf. Comput.* **4** 383
- [7] de Vicente J I and Huber M 2011 Multipartite entanglement detection from correlation tensors *Phys. Rev. A* **84** 062306
- [8] Klöckl C and Huber M 2015 Characterizing multipartite entanglement without shared reference frames *Phys. Rev. A* **91** 042339
- [9] Tran M C, Dakić B, Arnault F, Laskowski W and Paterek T 2015 Quantum entanglement from random measurements *Phys. Rev. A* **92** 050301
- [10] Tran M C, Dakić B, Laskowski W and Paterek T 2016 Correlations between outcomes of random measurements *Phys. Rev. A* **94** 042302
- [11] Eltschka C and Siewert J 2020 Maximum N -body correlations do not in general imply genuine multipartite entanglement *Quantum* **4** 229
- [12] Wyderka N and Gühne O 2020 Characterizing quantum states via sector lengths *J. Phys. A: Math. Theor.* **53** 345302
- [13] Hein M, Eisert J and Briegel H J 2004 Multiparty entanglement in graph states *Phys. Rev. A* **69** 062311
- [14] Hein M, Dür W, Eisert J, Raussendorf R, Van den Nest M and Briegel H J 2006 Entanglement in graph states and its applications (arXiv:quant-ph/0602096)
- [15] Bouchet A 1993 Recognizing locally equivalent graphs *Discrete Math.* **114** 75
- [16] Van den Nest M, Dehaene J and De Moor B 2004 Graphical description of the action of local Clifford transformations on graph states *Phys. Rev. A* **69** 022316
- [17] Ji Z, Chen J, Wei Z and Ying M 2010 The LU-LC conjecture is false *Quantum Inf. Comput.* **10** 97
- [18] Tsimakuridze N and Gühne O 2017 Graph states and local unitary transformations beyond local Clifford operations *J. Phys. A Math. Theor.* **50** 195302
- [19] Miller D, Fischer L E, Sokolov I O, Barkoutsos P K and Tavernelli I 2022 Hardware-tailored diagonalization circuits (arXiv:2203.03646)
- [20] Huber F and Severini S 2018 Some Ulam's reconstruction problems for quantum states *J. Phys. A: Math. Theor.* **51** 435301

- [21] Huber F, Eltschka C, Siewert J and Gühne O 2018 Bounds on absolutely maximally entangled states from shadow inequalities and the quantum MacWilliams identity *J. Phys. A: Math. Theor.* **51** 175301
- [22] Greenberger D M, Horne M A and Zeilinger A 1989 Going beyond Bell's theorem *Bell's Theorem, Quantum Theory and Conceptions of the Universe* vol 69, ed M Kafatos (Kluwer)
- [23] Miller M and Miller D 2021 GraphStateVis: interactive visual analysis of qubit graph states and their stabilizer groups *IEEE Trans. Quantum Eng.* **1** 378
- [24] Jungnitsch B, Moroder T and Gühne O 2011 Entanglement witnesses for graph states: general theory and examples *Phys. Rev. A* **84** 032310
- [25] Raussendorf R, Browne D E and Briegel H J 2003 Measurement-based quantum computation on cluster states *Phys. Rev. A* **68** 022312
- [26] Briegel H J, Browne D E, Dür W, Raussendorf R and Van den Nest M 2009 Measurement-based quantum computation *Nat. Phys.* **5** 19
- [27] Miller D 2019 Small quantum networks in the qudit stabilizer formalism *Master's Thesis* (arXiv:1910.09551)
- [28] Royle G 2020 Graph that minimizes the number of b/w colorings where white vertices have an odd number of black (available at: mathoverflow.net/q/376673) (Accessed 22 June 2022)
- [29] Erdős P and Rényi A 1960 On the evolution of random graphs *Publ. Math. Inst. Hungary. Acad. Sci.* **5** 17
- [30] Knill E 2019 Non-binary unitary error bases and quantum codes *LANL Report LAUR-96-2717* (arXiv:quant-ph/9608048)
- [31] Gheorghiu V 2014 Standard form of qudit stabilizer groups *Phys. Lett. A* **378** 505
- [32] Grassl M, Klappenecker A and Rotteler M 2002 Graphs, quadratic forms, and quantum codes (arXiv:quant-ph/0703112)
- [33] Bahramgiri M and Beigi S 2006 Graph states under the action of local Clifford group in non-binary case (arXiv:quant-ph/0610267)
- [34] Yong Looi S Y and Griffiths R B 2011 Tripartite entanglement in qudit stabilizer states and application in quantum error correction *Phys. Rev. A* **84** 052306
- [35] Kaszlikowski D, Sen(De) A, Sen U, Vedral V and Winter A 2008 Quantum correlation without classical correlations *Phys. Rev. Lett.* **101** 070502
- [36] Miller D, Holz T, Kampermann H and Bruß D 2018 Propagation of generalized Pauli errors in qudit Clifford circuits *Phys. Rev. A* **98** 052316
- [37] Quek Y, Stilck França D, Khatri S, Jakob Meyer J and Eisert J 2022 Exponentially tighter bounds on limitations of quantum error mitigation (arXiv:2210.11505)
- [38] Grasselli F 2020 *Quantum Cryptography: From Key Distribution to Conference Key Agreement* (Springer)
- [39] Peres A 1996 Separability criterion for density matrices *Phys. Rev. Lett.* **77** 1413
- [40] Horodecki M, Horodecki P and Horodecki R 1996 Separability of mixed states: necessary and sufficient conditions *Phys. Lett. A* **223** 1
- [41] Bombin H and Martin-Delgado M A 2007 Optimal resources for topological two-dimensional stabilizer codes: comparative study *Phys. Rev. A* **76** 012305
- [42] Bravyi S, Englbrecht M, König R and Peard N 2018 Correcting coherent errors with surface codes *npj Quantum Inf.* **4** 55
- [43] Fowler A G, Mariantoni M, Martinis J M and Cleland A N 2012 Surface codes: towards practical large-scale quantum computation *Phys. Rev. A* **86** 032324
- [44] Van den Nest M, Dehaene J and De Moor B 2005 Finite set of invariants to characterize local Clifford equivalence of stabilizer states *Phys. Rev. A* **72** 014307
- [45] Cabello A, López-Tarrida A J, Moreno P and Portillo J R 2009 Compact set of invariants characterizing graph states of up to eight qubits *Phys. Rev. A* **80** 012102
- [46] Nielsen M A and Kempe J 2001 Separable states are more disordered globally than locally *Phys. Rev. Lett.* **86** 5184
- [47] Hein M, Dür W and Briegel H-J 2005 Entanglement properties of multipartite entangled states under the influence of decoherence *Phys. Rev. A* **71** 032350
- [48] Navascués M, Pironio S and Acín A 2008 A convergent hierarchy of semidefinite programs characterizing the set of quantum correlations *New J. Phys.* **10** 073013
- [49] Adesso G and Illuminati F 2007 Entanglement in continuous-variable systems: recent advances and current perspectives *J. Phys. A: Math. Theor.* **40** 7821

- [50] Sun Q and Zubairy M S 2012 Entanglement criteria for continuous-variable systems *Classical, Semi-Classical and Quantum Noise* ed L Cohen, H Poor and M Scully (Springer) pp 249–58
- [51] Rossi M, Huber M, Bruß D and Macchiavello C 2013 Quantum hypergraph states *New J. Phys.* **15** 113022
- [52] Meštrović R 2018 Several generalizations and variations of Chu-Vandermonde identity (arXiv:1807.10604)
- [53] Simon C and Kempe J 2002 Robustness of multiparty entanglement *Phys. Rev. A* **65** 052327
- [54] Terhal B M 2000 Bell inequalities and the separability criterion *Phys. Lett. A* **271** 319
- [55] Gühne O, Hyllus P, Bruß D, Ekert A, Lewenstein M, Macchiavello C and Sanpera A 2002 Detection of entanglement with few local measurements *Phys. Rev. A* **66** 062305
- [56] Bourennane M, Eibl M, Kurtsiefer C, Gaertner S, Weinfurter H, Gühne O, Hyllus P, Bruß D, Lewenstein M and Sanpera A 2004 Experimental detection of multipartite entanglement using witness operators *Phys. Rev. Lett.* **92** 087902
- [57] Gühne O and Tóth G 2009 Entanglement detection *Phys. Rep.* **474** 1
- [58] Gong M et al 2019 Genuine 12-qubit entanglement on a superconducting quantum processor *Phys. Rev. Lett.* **122** 110501
- [59] Wei K X, Lauer I, Srinivasan S, Sundaresan N, McClure D T, Toyli D, McKay D C, Gambetta J M and Sheldon S 2020 Verifying multipartite entangled Greenberger-Horne-Zeilinger states via multiple quantum coherences *Phys. Rev. A* **101** 032343
- [60] Mooney G J, White G A L, Hill C D and Hollenberg L C L 2021 Generation and verification of 27-qubit Greenberger-Horne-Zeilinger states in a superconducting quantum computer *J. Phys. Commun.* **5** 095004
- [61] Song C et al 2019 Generation of multicomponent atomic Schrödinger cat states of up to 20 qubits *Science* **365** 574
- [62] Liu Z and Fan H 2009 Decay of multiqubit entanglement *Phys. Rev. A* **79** 064305
- [63] Dür W, Vidal G and Cirac J I 2000 Three qubits can be entangled in two inequivalent ways *Phys. Rev. A* **62** 062314
- [64] Flammia S T and Liu Y-K 2011 Direct fidelity estimation from few Pauli measurements *Phys. Rev. Lett.* **106** 230501
- [65] Helwig W 2013 Absolutely maximally entangled qudit graph states (arXiv:1306.2879)
- [66] Eisenbud D 1995 *Commutative Algebra with a View Toward Algebraic Geometry* (Springer Graduate Texts in Mathematics vol 150) (Springer) (<https://doi.org/10.1007/978-1-4612-5350-1>)